SIMULATION AND OPTIMIZATION OF SUSPENSION PVC BATCH REACTOR

A Thesis Submitted

In Partial Fulfilment of the Requirements

for the Degree of

MASTER OF TECHNOLOGY

By

S. RAMESH CHANDRAN

to the

DEPARTMENT OF CHEMICAL ENGINEERING

INDIAN INSTITUTE OF TECHNOLOGY, KANPUR

June, 1993

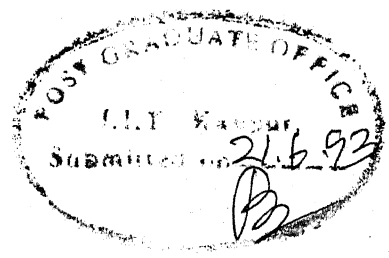

CERTIFICATE

This is to certify that the present work titled, **"SIMULATION AND OPTIMIZATION OF SUSPENSION PVC BATCH REACTOR"** by S. Ramesh Chandran has been carried out under my supervision and has not been submitted elsewhere for a degree.

Ashok Khanna

June 21 ,1993

Dr Ashok Khanna
Assistant Professor
Department of Chemical Engineering
Indian Institute of Technology
Kanpur - 208016
India

CHE-1993-M- CHA-SIM

ACKNOWLEDGEMENTS

I express my sincere gratitude to my guide Dr Ashok Khanna for his valuable suggestions and constant encouragement throughout this work.

I also thank all other faculties of the chemical engineering department for imparting a good knowledge of chemical engineering through their excellent teaching. In particular I am very much grateful to Dr Santosh K Gupta for enlightening me with various optimization techniques through his unique way of teaching.

I am very much thankful to all my friends especially to Mr R.Ramesh Rao, Mr N.Ravichander, Mr S.Sreenivasa Rao and Mr Sivakumar for providing me tips throughout the course and making my stay at IIT, Kanpur enjoyable. I also thank Mr Om Pal Singh for assisting me in completing this thesis. I thank Mr Venkatasubramanian for helping me in getting the print out amidst his tight work.

I am deeply indebted to my senior Mr J.Govindhakannan for guiding me in all aspects and confidence he had on me.

At last but not the least I thank Indian Petrochemicals Corporation Limited (IPCL), Vadodara for providing me the necessary data for simulation and partial financial support, given during this project.

Sundaram Ramesh Chandran.

CONTENTS

Abstract

A multiphase mathematical model for suspension polymerization of VCM in a batch reactor has been presented here. This model incorporates mass transfer for the initiator, monomer and radical species between the different phases involved (i.e., monomer, polymer, VCM droplet surface, aqueous and vapor phases). This includes the possibility of inhomogeneity of both the initiator distribution and initiator efficiency. The model accounts for precipitation of polymer from monomer phase and also the pressure drop in the reactor. The model has been modified to incorporate the continuous addition of seal and injection water in accordance with industrial practice. The model predicts the rate of polymerization, pressure drop in the reactor, instantaneous and cumulative molecular weight averages, short and long chain branching characteristics with respect to process conditions. The sensitivity of polymerization rate and pressure to various model parameters has been investigated. These sensitive parameters have been tuned with respect to industrial data. The parameters have been estimated using the simplex optimization technique. When the objective is to utilise the maximum cooling capacity of reactor the optimal temperature profile has been obtained by using Pontryagin's Principle. We have also estimated various heat transfer coefficients using industrial data.

LIST OF FIGURES

LIST OF TABLES

Nomenclature

A_{bf} baffle heat transfer area, dm^2

A_{ij} mass transfer area for the transfer from phase i to phase j, dm^2

A_{ja} jacket heat transfer area, dm^2

C_M heat capacity of the metal wall, J/gm K

C_p heat capacity of the reaction mixture, J/gm K

C_W heat capacity of the coolant water, J/gm K

D^y_{ij} diffusivity of species y from phase i to phase j, dm^2/sec

d_p diameter of the droplet, dm

D_R reactor diameter, dm

f_i initiator efficiency in phase i

F_I flow rate of initiator, gmol/sec

F_{Ii} flow rate of initiator into phase i, gmol/sec

F_M flow rate of monomer, gmol/sec

F_{Mi} flow rate of monomer into phase i, gmol/sec

h_{in} reactor inside heat transfer coefficient, W/dm^2 K

h_{ja} jacket heat transfer coefficient, W/dm^2 K

h_{bf} baffle heat transfer coefficient, W/dm^2 K

H_a heat developed by agitation, J/sec

H_R reactor height, dm

k^y_{Mij} mass transfer coefficient for species y from phase i to j, dm/sec

k_{di} initiator decomposition rate constant,in phase i, sec^{-1}

k_{pi} propagation rate constant in phase i, dm^3/gmol sec

k_{trMi} rate constant for chain transfer to monomer in phase i, dm^3/gmol sec

k_{trPi}	rate constant for chain transfer to polymer in phase i, dm^3/gmol sec
k_{ti}	termination rate constant, dm^3/gmol sec
$\dot{m}_{ja}$	coolant mass flow rate through jacket, gm/sec
$\dot{m}_{bf}$	coolant mass flow rate through baffle, gm/sec
M_O	initial charge of VCM, gmol
MW_I	molecular weight of initiator, gm/gmol
MW_M	molecular weight of VCM, gm/gmol
$\dot{q}_{iw}$	volumetric flow rate of injection water, dm^3/sec
$\dot{q}_{sw}$	volumetric flow rate of seal water, dm^3/sec
P_n	dead polymer having n repeating units
R_n	polymer radical having n repeating units
r_p	rate of polymerization, kg/sec
r_d	desired rate of polymerization, kg/sec
R_p	radius of polymer particle, dm
Sh	Sherwood number
T	reactor temperature, K
T_{ja}	temperature of coolant in the jacket, K
T_{jae}	exit temperature of coolant in the jacket, K
T_{jai}	inlet jacket coolant temperature, K
T_{bf}	temperature of coolant in the baffle, K
T_{bfe}	exit temperature of coolant in the baffle, K
T_{bfi}	inlet baffle coolant temperature, K
T_{m1}	jacket metal wall temperature, K
T_{m2}	baffle metal wall temperature, K
V_{fp}	free volume fraction of polymer
V_{fcr}	critical free volume fraction of polymer

V_{ja} volume of the jacket, dm^3

V_{bf} volume of the baffle, dm^3

V_{m1} volume of the jacket metal wall, dm^3

V_{m2} volume of the baffle metal wall, dm^3

V_R volume of reactor, dm^3

V_O initial volume of VCM, dm^3

x conversion

x_c critical conversion

Greek Letters

α gel phase rate enhancement

β initiator efficiency ratio

γ_{ij}^{y} partition coefficient for species y between phases i and j

ρ_m density of VCM, gm/dm^3

ρ_{mw} density of the metal wall, gm/dm^3

ρ_p density of the polymer, gm/dm^3

ρ_w density of the coolant water, gm/dm^3

$(-\Delta H)$ heat of the reaction, J/gmol

ξ flocculation coefficient

$\sigma_{0i}, \sigma_{1i}, \sigma_{2i}$ zeroth, first and second moments of polymer radical

$\lambda_{0i}, \lambda_{1i}, \lambda_{2i}$ zeroth, first and second moments of dead polymer

λ_i lagrangian multiplier for i^{th} state variable

Subscripts

i, j phase labels

0 initial value

1 monomer phase

2 polymer phase

3 VCM droplet phase

4 water phase

5 vapor phase

Superscripts

y species: initiator,monomer,polymer

CHAPTER 1

INTRODUCTION

1.1 Overview

Polyvinyl chloride (PVC) is one of the oldest thermoplastic polymers. The commercial production of PVC started in 1931 in Germany and it became commercially very significant prior to World War II. A major reason for the long delay between discovery and commercialisation was that unmodified PVC is not a useful material. A significant step in promoting the growth of PVC industry was the development of oxychlorination process which made it possible to use ethylene as feed stock for vinyl chloride monomer (VCM) production. Another major factor for the growth of PVC industry is that it is the largest consumer of chlorine,which is essentially a by-product in the manufacture of sodium hydroxide. Currently, next to polyethylene, PVC is the most frequently used thermoplastic material.

The commercial production of PVC is based on three processes: suspension,emulsion and bulk polymerization. The suspension process is the dominating route to PVC. It accounted for about 80% of world production in 1980. In India also,suspension process accounts for the major production capacity. The industries that manufacture PVC in India at present (1993) are Indian Petrochemicals Corporation Ltd, Chemicals and Plastics India Ltd, Reliance, Finolex, Shriram Plastics, etc..

The suspension process is favoured because of the relative ease of polymerization control (due to water acting as a large heat sink) and lower cost of separating and drying the resin. The

suspension process is carried out in a glass lined or highly polished stainless steel stirred tank batch reactor with a jacket,meant for heating and cooling. The raw materials used are Vinyl Chloride Monomer (VCM),demineralised water and certain additives including a suspension stabiliser. Polymerization of VCM is a free radical type of chain reaction. Once the batch attains the desired reaction temperature by heating,the polymerization reaction becomes self sustaining. It is exothermic in nature and heat has to be removed continuously for stable operation. The heat of reaction is removed through the jacket to bring the reactor contents to the desired polymerization temperature. Normally it takes 3-6 hrs to reach 85-90% conversion. The process is characterised by an auto-accelerating real time profile ,in some cases producing a marked peak near the end of the reaction,which can cause problems with temperature control and the danger of run away reaction.

The product quality of suspension PVC is, to a large extent, controlled by the particular suspension stabilizer system used and the precise manner in which the polymerization is carried out. The suspension stabilizer system affects the shape of the grains,the grain size distribution,resin porosity and bulk density of resin. Typical suspension stabilizers used in industry are methyl hydroxy propyl cellulose,poly vinyl alcohol etc.

1.2 Literature Survey

There has been considerable amount of work on the modelling [1-15] of PVC formation reported in the literature,particularly in developing kinetic mechanisms. These models are all based on

the key feature that PVC is essentially insoluble in its monomer so that as polymerization proceeds within the monomer droplets,solid polymer precipitates out and swells to the extent of approximately 23% by weight of VCM to form a deformable viscoelastic gel.

1.2.1 Two Phase Model

Talamini [1] were the first to derive a two phase (monomer rich phase and polymer rich phase) model to predict the time variation of fractional monomer conversion in a suspension PVC batch reactor. The assumptions made in Talamini's model are

i) The corresponding initiator decomposition and propagation rate constants as well as the initiator efficiencies in the two phases are equal

ii) The initiator concentration is the same in both the phases.

iii) No transfer of radicals between two phases occurs.

iv) The initiator concentration does not change with conversion.

v) The volume of the reaction mixture remains constant.

This was the first model to predict the rate of polymerization up to 70% conversion. The onset of two separate phases was reported to begin after less than 1% conversion and lasts until between 70-80% conversion. This particular conversion at which the monomer phase gets depleted is called the critical conversion x_c.

Abdel-Alim and Hamielec [2] modified Talamini's model by replacing assumptions (iv) and (v) with the following assumptions:

vi) The initiator concentration changes with reaction time.

vii) The volume of the reaction mixture varies linearly with

conversion.

This model assumes the presence of two phases in equilibrium,each of constant composition (x_1 & x_2 % of polymer respectively). x_1 is very small,so taken as zero,that is,the monomer rich phase contains only monomer. This model could also predict the molecular weight distribution (MWD) throughout the entire range of conversions and has been applied to commercial PVC processes.

Ugelstad [3] assumed production of radicals in both phases in contrast to Abdel-Alim and Hamielec model. They also included the transfer of radicals between the two phases. However,they suggested that an equilibrium distribution of radicals is quickly established between the two phases,which means no net transfer of radicals takes place between the phases. Ugelstad [4] and Olaj [5] have put considerable efforts into refining the kinetic mechanism of the process,but have tended to concentrate on the low conversion behaviour. Kuchanov and Bort [6] assumed that the radical transfer from polymer phase can be completely neglected. Whilst these earlier models recognised the existence of the two distinct phases in the polymerization,they do not consider the detailed physical nature and structure of these phases.

1.2.2 Multiphase Model

Kelsall and Maitland [7] proposed a multiphase mass transfer model (monomer, polymer, VCM droplet surface, aqueous, and vapor phases), incorporating: (a) mass transfer for various species within the different phases involved, and (b) inhomogeneous initiator distribution between monomer and polymer phase and (c) initiator efficiency ratio between monomer and polymer phase. The

model can predict rate profile, and several important properties of product like porosity,apparent density and particle size etc. from a knowledge of process conditions. But this model does not account for diffusion controlled propagation , termination rate constants at high monomer conversions and transfer to polymer.

1.2.3 At High Conversions (beyond x_c)

Many workers [8-15] have studied experimentally the polymerization of vinyl chloride. Xie [8] experimentally investigated the vinyl chloride polymerization at high conversion and reported that reactor pressure falls before monomer is completely consumed and the conversion at which pressure drops depends on the morphology of the PVC particles. They have surmised that reactor pressure falls in two stages. The first stage is due to the volume increase of the vapor phase as a result of volume shrinkage during reaction. The monomer phase has not yet been consumed at this stage but is trapped in the interstices between primary particles creating a mass transfer resistance;therefore the pressure drops slowly. The second stage is due to both the volume increase of vapor phase and to the monomer in the vapor phase diffusing into polymer phase. They have said that the thermal stability and porosity of PVC product decreases significantly with conversion beyond the critical conversion.

Xie [9] proposed an equilibrium model relating temperature,pressure,monomer conversion,and monomer phase distribution for vinyl chloride polymerization. This model can be used to determine the monomer conversion beyond the pressure drop

by measurement of reactor temperature and pressure. Various assumptions have been incorporated into this model like vapor phase inside the reactor follows ideal gas law and the solubility of VCM in water follows Henry's law.

Hamielec [10] first applied the free volume theory to model diffusion-controlled termination and propagation to explain the properties of PVC obtained at high conversions, which has been utilised by Xie [11]. These modelling attempts were premature due to inadequate amount of kinetic data at these high conversion levels.

1.2.4 Semi-batch Operation

Xie [12] has developed a semi-batch reactor model for suspension polymerization of vinyl chloride. In the conventional batch process, at high conversions (conversion > x_c), the kinetic behaviour of VCM polymerization changes with conversion dramatically, and this includes changes in reactor pressure, monomer concentration, reactor rate, instantaneous and accumulated molecular weight averages. Also,properties of PVC, such as thermal stability, deteriorate with increasing conversion. All the kinetic features like decrease in decomposition rate constants, propagation rate constants, efficiency factor, and increase in chain transfer to monomer rate constants which occurs at high conversions can be attributed to the decrease in monomer concentration. He has found experimentally that these changes are minimized if a constant monomer concentration is maintained at high conversions by semi-batch operation. Also thermal instability of PVC is found to

be minimized at high conversions by keeping monomer concentration constant.

1.2.5 Polymer Properties and Thermal Stability

The effect of polymerization conditions on polymer properties have been investigated by the same authors [13] and they have found that thermal stability of PVC decreases with increase in polymerization temperature and the reactions forming defect structures are favoured at low monomer concentrations. Thermal instability of PVC is attributed to the formation of allylic and tertiary chlorine which becomes prominent after x_c. They have experimentally found out that dehydrochlorination rate increases as conversion increases beyond x_c, but it is independent of conversion below x_c. It also increases as temperature is increased. They have suggested, therefore, the most effective way to minimize the formation of defective structures is to maintain monomer concentration as high as possible during polymerization after pressure drop.

The most recent study on modelling of PVC suspension process was done by Sidiropolou and Kiparissides [14], where they used a similar approach as used by Kelsall and Maitland [7]. This model can give some new results like,the number of short and long chain branching as well as the number of unsaturated terminal double bonds per polymer molecule. This new approach may be useful for commercial PVC production.

Xie [11] has studied the kinetics and mechanism of vinyl chloride polymerization in detail from both chemical and physical point of view. He has said that chain transfer to monomer plays a

vital role in controlling molecular weight development in VCM polymerization. Also, the limiting size of the primary particle is approximately 1.4μm in diameter and the final number of primary particles is around $2.0*10^{11}$ cm^{-3} but is a function of reaction temperatures.

The molecular weight development during the suspension polymerization of VCM has been investigated by Xie [15]. He states that at high conversions the number average molecular weight decreases significantly as compared to weight average molecular weight consequently increasing the polydispersity index. The molecular weight of PVC increases significantly with decrease in polymerization temperature.

1.2.6 Optimization

Albright and Soni [16] have investigated the suspension PVC polymerization with multiple initiators. They say by using a mixture of fast and slow initiators, it is possible to get a completely flat rate profile. Economic saving of at least 10 - 30% can be realized by changing to initiators causing flatter rate of heat release. Large economic savings are also possible if a reflux condenser can be used to remove a portion of heat of reaction and of agitation from the reactor. The same authors [17] have developed a computer program for determining the optimum design of suspension PVC batch reaction system. Their model calculates design and key operating variables, number of reactors required for given annual production rates, capital costs, and operating costs.

1.2.7 Diffusivity

Berens [18] has investigated the diffusion process of VCM in PVC. He has found by experiments that initially for short time fickian diffusion takes place and later on the relaxation by swelling dominates thus producing non - fickian diffusion.

1.3 Morphology of PVC

The suspension process produces a particulate, free flowing product having the same general appearance with a mean particle size usually in the range 100-150μm.

Suspension polymers are usually porous in nature and made up of a large number of much smaller particles. Suspension PVC particles usually possess a pericellular skin or membrane which extends almost continuously over the entire outer surface of particle. This skin is known [19] to form during the early stages of polymerization (< 5% conversion) and this has been shown to be a PVA/PVC graft copolymer . It has been postulated [20] that the skin is formed by primary particles that, when first generated, are brought to monomer/water interface of dispersed droplets by centrifugal forces. They then destabilise, such that they fuse and form a continuous boundary that eventually grows to a thickness of about 1μm. As conversion rises the skin becomes rigid depending on the recipe used. Varying levels of coalescence within the skin now take place over the range of conversion 5 - 15% [21]. At a conversion close to critical conversion, the PVC internal structure and the skin surrounding the particles becomes rigid enough to give a significant resistance for monomer diffusion from vapor phase to polymer phase [8].

The morphological properties of the suspension PVC grains include shape, size & its distribution, surface characteristics internal structures and porosity. Among them, the size and its distribution, as well as porosity have crucial influence on the separation of free unreacted VCM from the grains and on the processing and the end use of these resins.

Process Variables Affecting the Particle Properties of Suspension PVC

1.3.1 Polymerization Temperature

In the absence of other reactive agents, the molecular weight of PVC is almost entirely determined by polymerization temperature [19]. Increasing the polymerization temperature in a reactor reduces the colloidal stability of domains and causes earlier aggregation. The size of primary particles increases and the number decreases, which leads to the formation of weaker networks of aggregates, less able to resist droplet contraction, and consequently grains with lower porosity are produced.

1.3.2 Conversion

Conversion is found to have a very large effect on product properties. In the range of conversions commonly encountered commercially (i.e., 75-95%) porosity is generally found to decrease with increasing conversion. This is because very low conversion products, lacking in internal strength collapse inwardly on themselves thus reducing porosity and increasing bulk density.

1.3.3 Dispersant

The polymerising monomer droplets in the suspension process are formed and stabilised by the combined effect of vigorous agitation and the presence of a dispersant or dispersants. The choice of the dispersant is of utmost importance as it not only contributes to controlling the particle size distribution of PVC produced but also has a major effect on the sub-structure of the particle in terms of its porosity etc.

1.3.4 Agitation

Agitation is of fundamental importance in the suspension PVC process. Together with the dispersant system it governs the stability of the suspension during polymerization and the particle size of the product formed. Agitation can also have an important role in determining other product properties such as porosity and bulk density.

In an agitated dispersion, the turbulent velocity fluctuations through out the mixing tank tend to bring about separation of all adhering droplet clusters during the critical time period, so that the chance of coalescence is minimal. Both the force of adhesion between droplets and the forces caused by agitation (which tend to separate the droplets) depend on the diameter of the droplet. However, the changes of separation are greater the larger the droplets and thus, for a given level of agitation, there exists a minimum droplet diameter above which stabilisation by agitation becomes possible. By contrast, the susceptibility towards droplet break-up, caused by local velocity fluctuations and shear forces near the impeller, is increased by

increases in droplet size. The minimum droplet size that is able to remain stable to break-up will, of course, increase with decreasing agitator speed. However, in the case of very low agitation intensity large droplets may become unstable due to phase separation cause by specific gravity differences.

Increased severity of agitation is often found to increase porosity although this does not appear to always be the case. Hofmann [22] in fact found an initial reduction in porosity with increasing agitator speed followed by an increase corresponding to the increase in particle size observed. He attributes the increase in product porosity that occurred under high agitation conditions to two factors. Firstly, the increased degree of agglomeration results in the formation of a greater number of voids at the interstices between the discrete particles. Secondly, increased porosity is said to occur due to the internal structure of the primary particle being disturbed, with the membranes of the individual polymerising droplets being torn and partially destroyed by the agglomeration process.

1.3.5 Other variables

Water : monomer phase ratio is often considered an important production parameter in suspension polymerization. Certainly in the case of vinyl chloride polymerization there are physical limitations to the minimum phase ratio. A very low proportion of water will cause instability and gross distortion of the particle size distribution. At a level somewhat higher than this, depending on resin porosity, problems are encountered due to absorption of water within the grains causing a drying out effect

and thus high slurry viscosities. This effect can be overcome by adding extra water during polymerization.

The presence of even trace quantities of oxygen during the polymerization can have dramatic effects on both the chemical and physical properties of the resulting PVC. The most obvious effect is that on particle size which is decreased considerably as the reactor oxygen content is increased.

Cebollada [23] has found by experiments that molecular weight of PVC remains insensitive to changes in viscosity of the suspension medium. For all practical purposes, viscosity bears no influence on the reaction kinetics. But it plays a fundamental role in the determination of particle size distribution. High viscosity media produce larger size, unicellular spherical particles retaining their identity as individual droplets. Conversely, low viscosity media favor the formation of smaller particles.

The processing characterstics of suspension PVC are largely determined by the molecular weight of the polymer and morphology of the grains [24]. As molecular weight is reduced, the viscosity of the hot melt decreases and polymer becomes easier to process, although the strength of the finished article is reduced.

1.4 Proposed Objectives

The objectives of the present work are the following:

a) To simulate the multiphase mass transfer model for suspension PVC polymerization process in a batch reactor.

b) To find out what model parameters are sensitive to rate of polymerization and pressure drop in the reactor.

c) To estimate the aforementioned parameters using industrial data.

d) To estimate the heat transfer coefficients from the industrial data.

e) To find out the optimal temperature policy for maximum utilisation of cooling capacity of the reactor.

f) To predict instantaneous and cumulative molecular weight averages.

g) To use semi-batch mode of operation with respect to monomer after critical conversion to keep the pressure constant, reduce the thermal instability, and to increase the productivity.

CHAPTER 2

MULTI-PHASE MODEL DEVELOPMENT

2.1 The Suspension Process

Before giving the details of the model,let us see the salient features of suspension PVC process it attempts to simulate.

The reactor considered here is a $70m^3$ reactor. The initiator used is 2-ethyl hexyl peroxydicarbonate (EHP). VCM and DM water (demineralised water) are added simultaneously into the reactor. EHP is then added over a short time. During polymerization seal water is added continuously in to the reactor to prevent the back flow and injection water is added to maintain the liquid volume constant. The excess heat from the reactor is removed by two ways. Coolant water is circulated through the half pipe jacket and the chilled water is circulated through the baffles inside the reactor. There are four baffles in the reactor with two concentric pipes where coolant flows from bottom to top in the inner pipe and drains out in the outer pipe. The schematic diagram of the reactors are shown in Fig 2.1a and Fig 2.1b.

PVC polymerization can be visualised in two ways: one is macroscopic scale and the other is the microscopic scale.

Macroscopic Scale : An aqueous suspension of VCM droplets at a volume fraction of approximately 40 is formed in the autoclave by vigorous agitation. The initial droplets are typically 50-150μm in diameter and are stabilised by the addition of a protective coalescence. Depending on the nature of the agitation and the degree of stabilisation,the polymerizing droplets may aggregate to a certain extent as conversion increases to produce

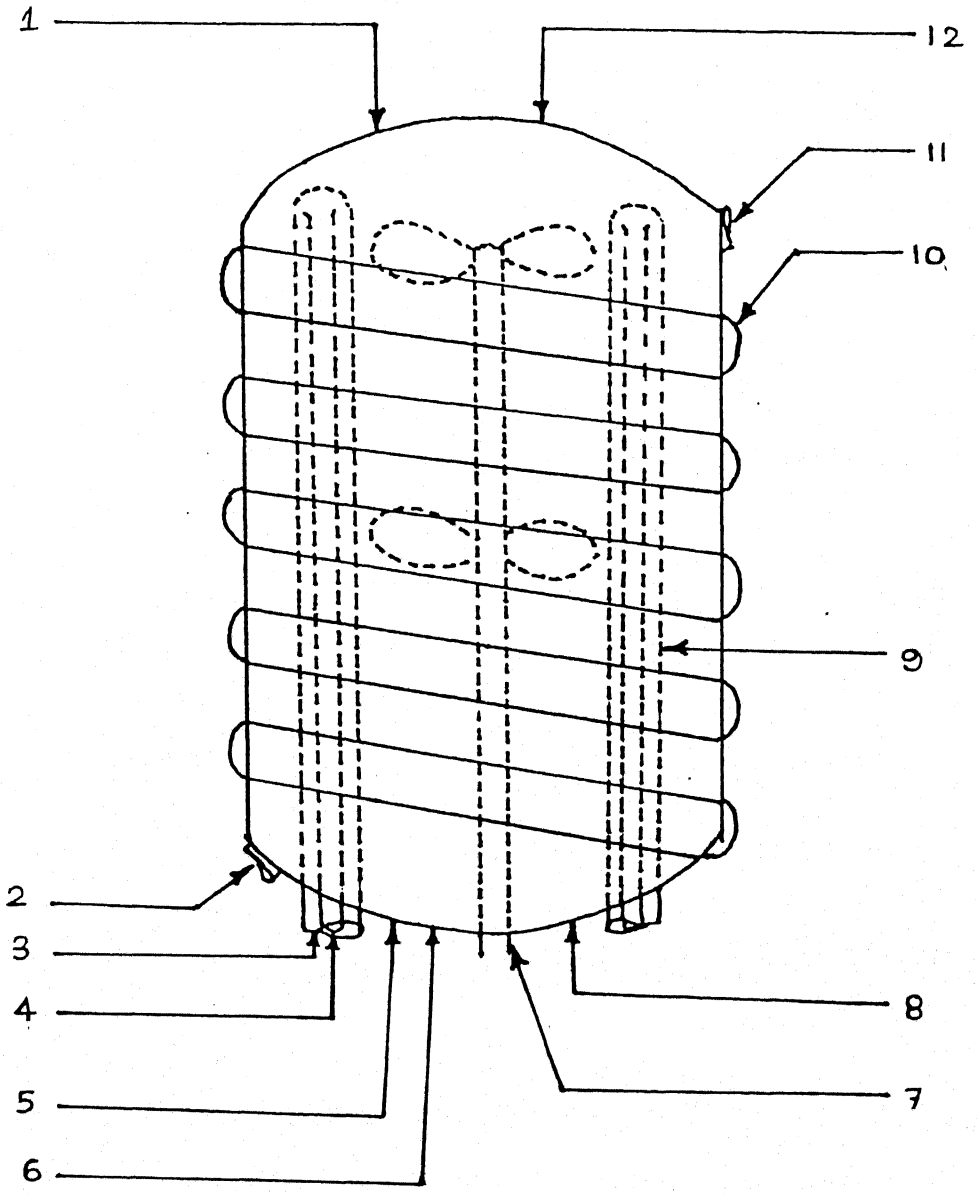

Fig 2.1a Schematic Representation of the Reactor.

1	VCM charge	7	Agitator
2	Jacket coolant inlet	8	Injection water addition
3	Baffle coolant outlet	9	Baffles
4	Baffle coolant inlet	10	Half pipe jacket coil
5	Seal water addition	11	Jacket coolant outlet
6	DM water charge	12	Initiator charge

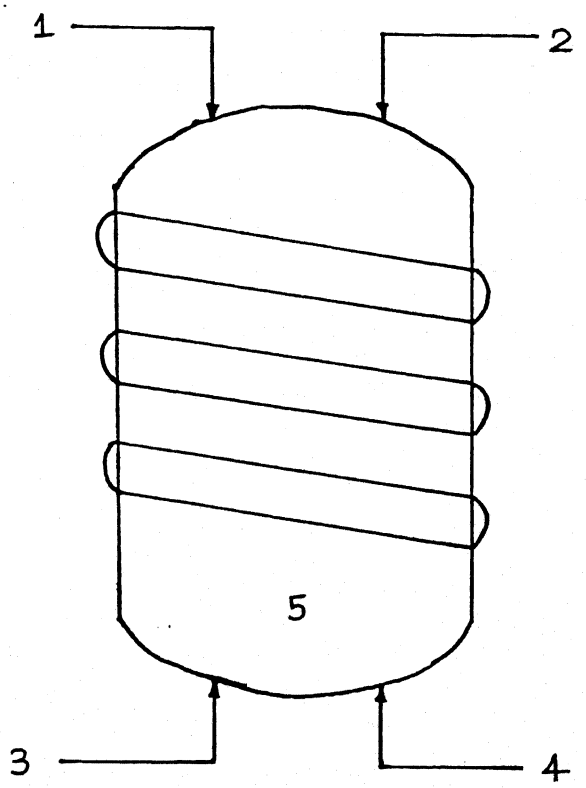

Fig 2.1b Schematic Representation of Semi-batch Reactor

1. F_M - Flow rate of monomer
2. F_I - Flow rate of initiator
3. $\dot{q}_{sw}$ - Volumetric flow rate of seal water
4. $\dot{q}_{iw}$ - Volumetric flow rate of injection water
5. Initial charge - VCM, DM water, buffer, and additives

a final particle (grain) of approximately 50-150μm. In addition, agitation must give adequate heat transfer from the droplets to ensure uniform temperature control.

Microscopic Scale : Superimposed upon this droplet aggregation process, another sequence takes place within each droplet. The growing chain radicals become insoluble in VCM at relatively short chain lengths (approximately 10 monomer units) and continue to grow as precipitated coiled macro-radicals. The first chains so formed aggregate in units of about 50 to produce small particles called micro-domains of diameter 200A°. These in turn flocculate to produce domains or primary particle nuclei (0.1 to 0.2μm) by 1% conversion. All growing macro-radicals and dead polymer chains are now absorbed by these units before they have a chance to nucleate fresh micro-domains and for the period the total number of domain particles remains constant, and they simply grow in size. These primary particles (0.2-0.4μm) eventually become unstable and flocculate, from about 3% conversion onwards, to form close-packed agglomerates of 1-2μm diameter. The way in which these units grow and pack together within the droplet is crucial for the development of both the reaction rate, grain porosity and apparent density. These primary particle aggregates continue to grow up to 10μm in diameter by surface deposition and internal growth, with increasing intra-primary growth, until polymerization is terminated at typically 90-95% conversion. This sequence of microscopic growth, which determines the essential characterstics of the final product, is summarised schematically in Fig 2.2.

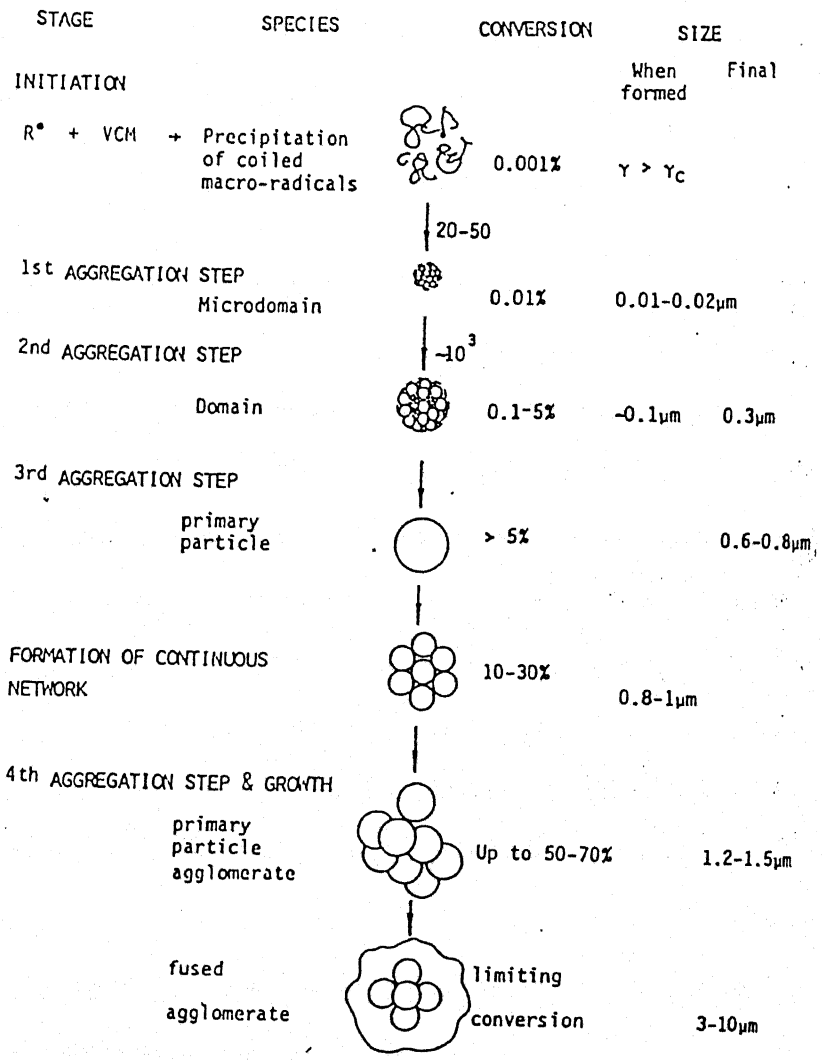

Fig 2.2 Scheme of PVC grain formation

2.2 Nature of Phases

A realistic model of the process should include polymerization within and mass transfer between all the phases. There are five phases, viz, monomer rich phase (phase 1), polymer rich phase (phase 2), VCM droplet surface phase (phase 3), aqueous phase (phase 4), and vapor phase (phase 5).

The major loci of polymerization are the two immiscible PVC/VCM phases.

Monomer Rich Phase

This is essentially pure monomer at conversions, less than 0.001;this is of course, the sole site of polymerization. This phase disappears at conversions approximately equal to 0.77,beyond which there is insufficient monomer to fully swell the formed polymer in polymer phase, and the autoclave pressure falls. The initiator is chosen to be highly soluble in this phase;chain radicals initiated here will precipitate out as soon as they grow more than a few monomer units into polymer phase. These precipitated chains are designated as phase 1 chains as long as they continue to grow,transfer to monomer or terminate by combination/disproportionation with another radical whilst suspended in phase 1. On adsorption by the phase 2 primary particles they become phase 2 radicals.

Polymer Rich Phase

This has an equilibrium composition of 0.77 mass fraction of polymer and 0.23 mass fraction of monomer and exists as highly deformable primary particles which grow and coalesce in manner described in section 2.1. The high density of chains in this phase has the effect of significantly reducing the rate at which

the end segments of the growing chain radicals can diffuse towards one another and couple to produce a dead chain. The simplest way to model this is an overall reduction in the effective rate constant for chain termination. The initiator is usually highly soluble in this phase also,but not necessarily to the same extent as in the phase 1. The creation of dead polymer is therefore accompanied by the transfer of both monomer and initiator from phase 1. Polymerization in phase 2 therefore occurs through (a) chains which were initiated in phase 1 and have migrated in to the phase 2 prior to termination or transfer and (b) chains which have been initiated in phase 2. There is evidence [25] that the rate of initiation process can be significantly lower than that in the phase 1.

VCM Droplet Surface

Electron microscopy studies [26] indicate that the surface region or skin of the initial subgrains is significantly different from the bulk in that the number density of primary particles is higher here,leading to an enhanced rate of polymerization in the early stage of process. In addition,the chemical nature of the polymer formed in this surface region can vary by incorporation of the adsorbed surfactant to form a graft copolymer. Both these factors contribute to the subgrain surface attaining a coherent close packed structure far earlier in the polymerization than the bulk.

Aqueous Phase

This phase fulfils the major role of providing a large heat sink through which the heat released by polymerization may be transfered to the autoclave wall. Although the solubilities of

VCM and initiator in water are both small,they may be significant in a full treatment,both in terms of polymerization and particularly,in affecting the rates of mass transfer of these species in to the polymerizing grains.

Vapor Phase

A few percent of the VCM in the autoclave resides in the vapor phase. This mass increases slightly as polymerization proceeds due to the volume decrease of the condensed phase. After pressure drop this remains as the sole reservoir of free monomer available to swell the gel phase;the rate of transfer of this monomer through phase 4 to the polymerization zone can greatly influence the rate of pressure drop.

2.3 Kinetic Mechanism

The kinetic mechanism of VCM polymerization has been investigated in much detail, and comprises many side reactions. In this work a simplified mechanism has been used, and the kinetic scheme is given in Table 2.1. The various options of reactions and mass transfers taking place in different phases is shown in Fig 2.3.

2.3.1 Kinetic Parameters

The kinetic parameters used in our model is given in Table 2.2. Although Hamielec [10] has reported that initiator decomposition rate constants, initiator efficiency, and chain transfer to monomer decreases with conversion after x_c, when we used his rate constant equations our model did not produce satisfactory results. It produced a steep fall in polymerization rate at high conversions.

Fig 2.3 Options for reaction and mass transfer within and between different phases

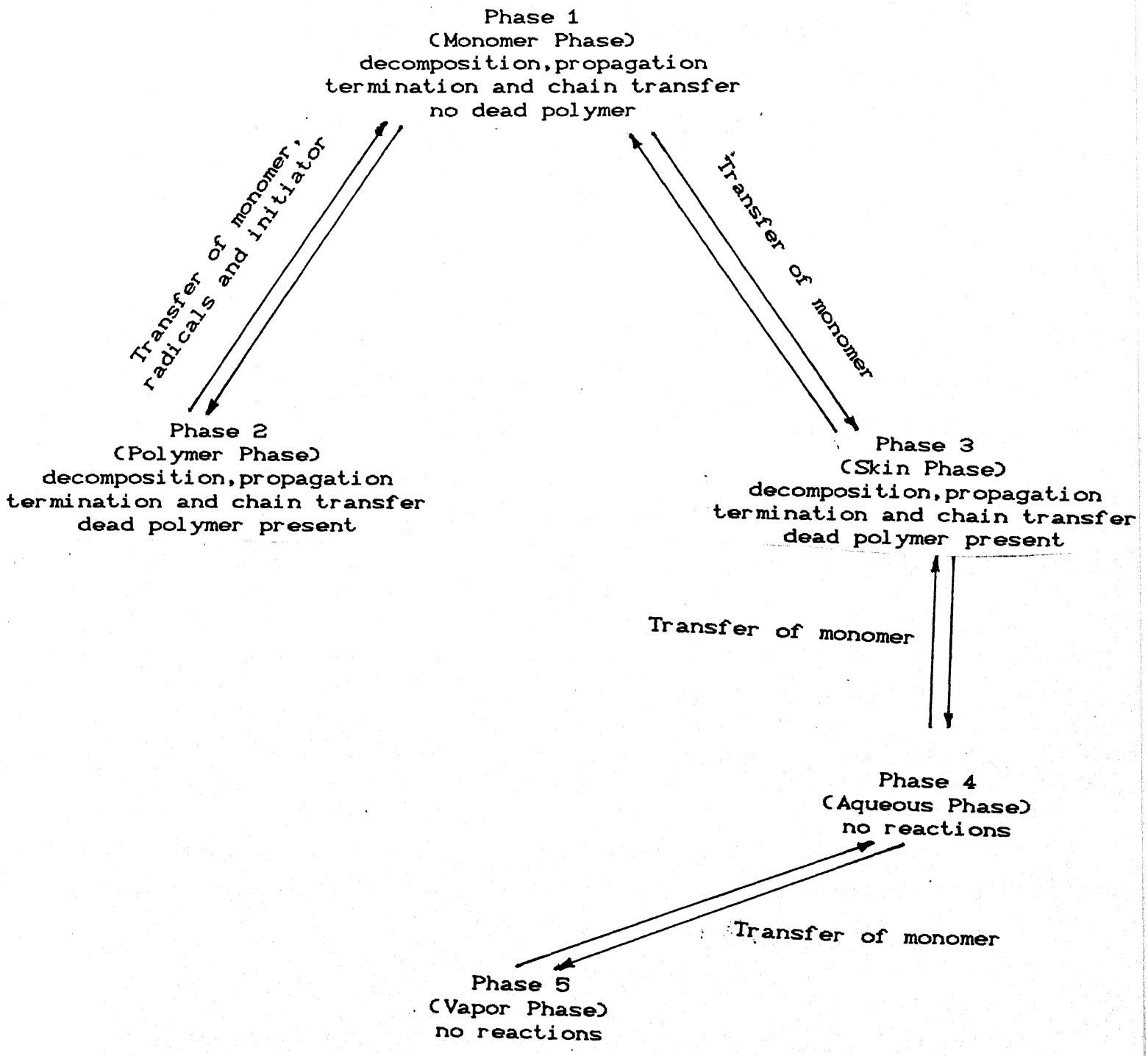

Table 2.1

Kinetic Scheme for Vinyl Chloride Polymerization

Initiation:

$$I_2 \xrightarrow{k_{di}} 2R_1 \qquad r_{di} = 2f_i k_{di} [I_2]$$

Propagation:

$$R_n + M \xrightarrow{k_{pi}} R_{n+1} \qquad r_{pi} = k_{pi} [R_n] [M]$$

Chain transfer to monomer:

$$R_n + M \xrightarrow{k_{trMi}} P_n + R_1 \qquad r^M_{tri} = k_{trMi} [R_n] [M]$$

Chain transfer to polymer:

$$R_n + P_m \xrightarrow{k_{trPi}} P_n + R_m \qquad r^P_{tri} = k_{trPi} [R_n] [P_m]$$

Termination:

$$R_n + R_m \xrightarrow{k_{ti}} P_n + P_m \quad (\text{or } P_{n+m}) \qquad r_{pi} = k_{ti} [R_n] [R_m]$$

i refers to the i^{th} phase, $i = 1, 2, \ldots, 5$

TABLE 2.2

Kinetic Rate Constants Used in the Model

Two options for using various kinetic rate constants are given below,

i) Decomposition rate constants		Ref
$k_{d1} = 1.5*10^{15} \exp(-14554.0/T)$		
$k_{d2} = k_{d1}$	at any x	[14]
(or)		
$k_{d2} = k_{d1}$	$x \leq x_c$	
$k_{d2} = k_{d1} \exp\{-C^*(1.0/V_{fp} - 1.0/V_{fx_c})\}$	$x > x_c$	[11]
where $C^* = 477.0 \exp(-2291/T)$		
ii) Propagation rate constants		
$k_{p1} = 5.0*10^{7} \exp(-3320/T)$		
$k_{p2} = k_{p1}$	$x \leq x_c$	
$k_{p2} = k_{p1} \exp\{-0.2(1.0/V_{fp} - 1.0/V_{fx_c})\}$	$x > x_c$	[14]
(or)		
$k_{p2} = k_{p1} \exp\{-B^*(1.0/V_{fp} - 1.0/V_{fx_c})\}$	$x > x_c$	[10]
where $B^* = 1.85*10^{13} \exp(-2595/T)$		
iii) Termination rate constants		
$k_{t1} = 1.3*10^{12} \exp(-2190/T)$		
$k_{t20} = k_{t1}/\alpha^{2.0}$	$x \leq x_c$	
$k_{t2} = k_{t20}\{(1 - x_c)/(1 - x)\}^{2.0} (k_{p2}/k_{p1})^{2.0}$	$x > x_c$	[14]
where $\alpha = 27.0 - 0.14\,(T - 273)$		
(or)		
$k_{t2} = k_{t1} \exp\{-A^*(1/V_{fp} - 1/V_{fcr})\}$	at any x	[10]
where $A^* = 6.64*10^{6} \exp(-4986/T)$		

iv) Chain tranfer rate constants

For monomer ,

$$k_{trM1} = 5.78 \exp(-2768/T)\, k_{p1}$$

$$k_{trM2} = k_{trM1} \qquad \text{at any } x \qquad [14]$$

(or)

$$k_{trM1} = 2262.5 \exp(-4262.0/T)\, k_{p1}$$

$$k_{trM2} = 827.11 \exp(-4476.83/T)\, k_{p2} \qquad x \le x_c$$

$$k_{trM2} = \frac{K_1}{1 + \frac{K_4}{K_5}[M_2]} \qquad x > x_c \qquad [15]$$

where $K_1 = (K_1)_{x_c} \exp\{-CH^*(1/V_{fp} - 1/V_{fx_c})\}$

$CH^* = 1.28*10^4 \exp(-3250/T)$

$(K_1)_{x_c} = 5.55*10^{12} \exp(-9340/T)$

$(K_4/K_5) = (K_4/K_5)_{x_c} \exp\{(-B^*(1/V_{fp} - 1/V_{fx_c})\}$

$(K_4/K_5)_{x_c} = 4260 \exp(-3410/T)$

For polymer,

$$k_{trP1} = 0.32\, k_{trM1}$$

$$k_{trP2} = k_{trP1} \qquad \text{at any } x \qquad [14]$$

(or)

$$k_{trP1} = 8.31*10^9 \exp(-11100/T)\, k_{p1}$$

$$k_{trP2} = k_{trP1} \qquad \text{at any } x \qquad [15]$$

v) Initiator efficiency factor

$$f_1 = 1.0$$

$$f_2 = 0.1 - 1.0 \qquad \text{at any } x \qquad [7]$$

(or)

$$f_1 = 1.0$$

$$f_2 = 0.1 - 1.0 \qquad x \le x_c$$

$$f_2 = \langle (k_{p2} f_2^{0.5})_{at\ x_c} \exp [-B_f^* (1/V_{fp} - 1/V_{fx_c})] \rangle^2 / k_{p2}^2$$

$$x > x_c \qquad [11]$$

where $B_f^* = 4.01 * 10^4 \exp (-3464/T)$

In the above equations V_{fp} and V_{fcr} are the free volume fraction of polymer and crtitical free volume fraction of polymer at which conversion, termination rate constant become diffusion controlled respectively. V_{fp} is calculated as follows,

$$V_{fp} = -0.416\ x + 0.42642 \qquad [14]$$

$$V_{fx_c} = V_{fp} \text{ at } x_c$$

The initiator efficiency ratio β is given as

$$\beta = \frac{f_2}{f_1} \qquad (2.1)$$

where f_1 and f_2 are initiator efficiencies in phase 1 and phase 2 respectively.

2.3.2 Physical Parameters

a) Partition coefficient for the species y between phases i and j

$$\gamma^{y}_{ij} = \left(\frac{[y_i]}{[y_j]}\right)_{eq} \qquad (2.2)$$

$$\text{e.g} \qquad \gamma^{I}_{12} = \frac{[I_1]_{eq}}{[I_2]_{eq}}$$

$$\text{and } \gamma^{y}_{ij} = \frac{1}{\gamma^{y}_{ji}} \qquad (2.3)$$

b) Rate of mass transfer of species y from phase i to phase j

$$= k^{y}_{Mij}\, A_{ij}([y_i] - [y_i]_{eq})$$

$$= k^{y}_{Mij}\, A_{ij}\left(\frac{y_i}{V_i} - \frac{\gamma^{y}_{ij}\, y_j}{V_j}\right) \qquad (2.4)$$

Since $[y_i]_{eq}$ is not known, it has been replaced by $\gamma^{y}_{ij}\,[y_j]$ i.e $\frac{\gamma_{ij}\, y_j}{V_j}$ in above equation, can be a good estimate of $[y_i]_{eq}$. When $[y_j]$ approaches its equilibrium value, the driving force under equilibrium is approached.

2.3.3 Moments and Molecular Weights

The chain length changes during polymerization are characterized in terms of the moments of the growing chain length

distribution σ_k, and of the dead polymer chain length distribution λ_k. σ_k and λ_k are defined by

$$\sigma_k(t) = \sum_{n=1}^{\infty} n^k R_n(t) \quad ; \quad \lambda_k(t) = \sum_{n=1}^{\infty} n^k P_n(t) \qquad (2.5)$$

The number and weight average molecular weights, $\bar{M}_n$ and $\bar{M}_w$, of dead polymer up to any time t are given by

$$\bar{M}_n = \frac{\lambda_1}{\lambda_0} MW_m \qquad \bar{M}_w = \frac{\lambda_2}{\lambda_1} MW_m \qquad (2.6)$$

$$\text{Polydispersity index , PDI} = \frac{\bar{M}_w}{\bar{M}_n} \qquad (2.7)$$

where MW_m is the monomer molecular weight.

2.3.4 Mole Balance Equations

Transformations of the mass balance for the various components involved in the polymerization using the generating function approach results in the following system of differential equations which characterize the process,

$$\frac{dI_i}{dt} = -k_{di} I_i - \sum_{j=i}^{3} \left(\frac{I_i}{V_i} - \frac{\gamma^I_{ij} I_j}{V_j} \right) k_{Mij} A_{ij} + F_{Ii} \quad ; \quad i=1,2,3 \qquad (2.8)$$

where F_{Ii} is the flow rate of initiator into phase i

$$\frac{dM_i}{dt} = -(k_{pi} + k_{trMi}) \frac{M_i \sigma_{0i}}{V_i} - \sum_{j=i}^{5} \left(\frac{M_i}{V_i} - \frac{\gamma^M_{ij} M_j}{V_j} \right) k^M_{Mij} A_{ij} + F_{Mi} \qquad i=1,2,\ldots,5 \qquad (2.9)$$

where F_{Mi} is the flow rate of monomer into phase i

$$\frac{d\sigma_{0i}}{dt} = 2f_i k_{di} I_i - \frac{k_{ti}\,\sigma_{0i}^2}{V_i} - \sum_{j=i}^{3}\left[\frac{\sigma_{0i}}{V_i} - \gamma^R_{ij}\frac{\sigma_{0j}}{V_j}\right] k^R_{Mij}\,A_{ij} \qquad i=1,2,3 \qquad (2.10)$$

$$\frac{d\sigma_{1i}}{dt} = 2f_i k_{di} I_i + k_{trMi}\,M_i\left(\frac{\sigma_{0i} - \sigma_{1i}}{V_i}\right) + k_{pi} M_i \frac{\sigma_{0i}}{V_i} - k_{ti}\frac{\sigma_{1i}\,\sigma_{0i}}{V_i} - k_{trpi}\frac{\lambda_{0i}\,\lambda_{1i}}{V_i} + k_{trpi}\frac{\lambda_{1i}\,\sigma_{0i}}{V_i} \qquad i=1,2,3 \qquad (2.11)$$

$$\frac{d\sigma_{2i}}{dt} = 2f_i k_{di} I_i + k_{trMi}\,M_i\left(\frac{\sigma_{0i} - \sigma_{2i}}{V_i}\right) + k_{pi} M_i \frac{(2\sigma_{1i} + \sigma_{0i})}{V_i} - k_{ti}\frac{\sigma_{2i}\,\sigma_{0i}}{V_i} - k_{trpi}\frac{\lambda_{0i}\,\lambda_{2i}}{V_i} + k_{trpi}\frac{\lambda_{0i}\,\lambda_{2i}}{V_i} - \sum_{j=i}^{3}\left[\frac{\sigma_{2i}}{V_i} - \gamma^R_{ij}\frac{\sigma_{2j}}{V_j}\right] k^R_{Mij}\,A_{ij} \qquad i=1,2,3 \qquad (2.12)$$

$$\frac{d\lambda_{0i}}{dt} = k_{trMi}\,M_i\frac{\sigma_{0i}}{V_i} + k_{ti}M_i\frac{\sigma_{0i}^2}{V_i} + \nu_i\left(k_{trM1}M_1\frac{\sigma_{01}}{V_1} + k_{t1}M_1\frac{\sigma_{01}^2}{V_1}\right) \qquad \text{for } i=2,3 \qquad (2.13)$$

where $\nu_2 = \frac{V_2}{(V_2 + V_3)}$ and $\nu_3 = \frac{V_3}{(V_2 + V_3)}$. There is no dead polymer in phase 1. As soon as radicals gets terminated in phase 1, it precipitates into phase 2 and phase 3 based on the volume fraction of each phase.

$$\frac{d\lambda_{1i}}{dt} = k_{trMi}\,M_i\,\frac{\sigma_{1i}}{V_i} + k_{ti}\,\frac{\sigma_{0i}\sigma_{1i}}{V_i} + k_{trpi}\frac{\lambda_{0i}\,\sigma_{1i}}{V_i}$$

$$- k_{trpi}\frac{\lambda_{1i}\,\sigma_{0i}}{V_i} + \nu_i \left[k_{trM1} M_1 \frac{\sigma_{11}}{V_1} + k_{t1}\frac{\sigma_{01}\sigma_{11}}{V_1} + k_{trp1}\frac{\lambda_{01}\sigma_{11}}{V_1} - k_{trp1}\frac{\lambda_{11}\sigma_{01}}{V_1} \right] \quad \text{for } i=2,3 \qquad (2.14)$$

$$\frac{d\lambda_{2i}}{dt} = k_{trMi}\, M_i \frac{\sigma_{2i}}{V_i} + k_{ti}\frac{\sigma_{0i}\sigma_{2i}}{V_i} + k_{trpi}\frac{\lambda_{0i}\,\sigma_{2i}}{V_i}$$

$$- k_{trpi}\frac{\lambda_{2i}\,\sigma_{0i}}{V_i} + \nu_i \left[k_{trM1} M_1 \frac{\sigma_{21}}{V_1} + k_{t1}\frac{\sigma_{01}\sigma_{21}}{V_1} + k_{trp1}\frac{\lambda_{01}\sigma_{21}}{V_1} - k_{trp1}\frac{\lambda_{21}\sigma_{01}}{V_1} \right] \quad \text{for } i=2,3 \qquad (2.15)$$

2.3.5 Volume change

For the monomer, polymer and skin phases ;

$$\frac{dV_i}{dt} = \left[\frac{1}{\rho_m}\frac{dM_i}{dt} + \frac{1}{\rho_p}\left(\frac{d\sigma_{1i}}{dt} + \frac{d\lambda_{1i}}{dt}\right) \right] MW_m \qquad i=1,2,3 \qquad (2.16)$$

For the aqueous phase ;

$$\frac{dV_4}{dt} = \frac{1}{\rho_m}\frac{dM_4}{dt} MW_m + (\dot{q}_{sw} + \dot{q}_{iw}) \qquad (2.17)$$

where $\dot{q}_{sw}$ and $\dot{q}_{iw}$ are volumetric flow rate of seal and injection water respectively.

For vapor phase, by conservation of total volume we get,

$$\frac{dV_5}{dt} = -\sum_{i=1}^{4}\frac{dV_i}{dt} \qquad (2.18)$$

2.3 6 Conversion and Rate

Conversion of monomer into polymer can be estimated from the following differential equation

$$\frac{dx}{dt} = -\frac{1}{M_O}\sum_{i=1}^{5}\frac{dM_i}{dt} \qquad (2.19)$$

The rate of polymerization, r_p can be calculated from the following equation ,

$$r_p = \frac{dx}{dt} M_O \, MW_m \qquad (2.20)$$

where M_O is the total moles of monomer charged.

2.4 Molecular Weight Development

The phasewise instantaneous number and weight average molecular weights at any time are calculated as follows,

$$\bar{M}_{ni} = \frac{\lambda_{1i}}{\lambda_{Oi}} MW_m \qquad i=2,3 \qquad (2.21)$$

$$\bar{M}_{wi} = \frac{\lambda_{2i}}{\lambda_{1i}} MW_m \qquad i=2,3 \qquad (2.22)$$

$$W_i = \lambda_{Oi} \bar{M}_{wi} \qquad i=2,3 \qquad (2.23)$$

$$w_i = \left(\frac{W_i}{W_2+W_3}\right) \qquad i=2,3 \qquad (2.24)$$

Since there is no dead polymer in the phase 1, $\bar{M}_{n1}$ and $\bar{M}_{w1}$ are negligible.

The overall instantaneous number average molecular weight $\bar{M}_{nI}$ is given by

$$\bar{M}_{nI} = \frac{1.0}{\left(\frac{w_2}{\bar{M}_{n2}} + \frac{w_3}{\bar{M}_{n3}}\right)} \qquad (2.25)$$

The overall instantaneous weight average molecular weight $\bar{M}_{wI}$ is given by

$$\bar{M}_{wI} = (w_2 \bar{M}_{w2} + w_3 \bar{M}_{w3}) \qquad (2.26)$$

The cumulative number average molecular weight $\bar{M}_{nA}$ is given by

$$\frac{x_{tf}}{\bar{M}_{nA}} = \int_0^t \frac{dx}{dt} \frac{1}{\bar{M}_{nI}} dt \qquad (2.27)$$

where x_{tf} is the terminal conversion.

Similarly for weight average molecular weight $\bar{M}_{wA}$

$$\frac{x_{tf}}{\bar{M}_{wA}} = \int_0^t \frac{dx}{dt} \frac{1}{\bar{M}_{wI}} dt \qquad (2.28)$$

2.5 Interphase Constitutive Relations

Mass transfer coefficients have been calculated from Sherwood number estimates according to the following definition

$$\frac{k^y_{Mij}\, d_p}{D^y_{ij}} = Sh \qquad (2.29)$$

when Sh = 2.0 then

$$k^y_{Mij} = \frac{2.0\, D^y_{ij}}{d_p} \quad \text{or} \quad \frac{D^y_{ij}}{R_p}$$

where d_p and R_p are diameter of droplet and radius of particle. The relationship between the mass transfer coefficients k^y_{Mij} and k^y_{Mji} has been found out as [27]

$$k^y_{Mij} = \gamma^y_{ji}\, k^y_{Mji} \qquad (2.30)$$

These relations have been used mainly for estimating mass transfer coefficients.

The mass transfer areas A_{ij} are taken to be

$$A_{12} = (36\, \pi\, N\, V_0\, V_2)^{1/3} \qquad (2.31)$$

$$A_{13} = A_{34} = n\, \pi\, d_p^2 \qquad (2.32)$$

$$A_{45} = \pi\, R_A^2 \qquad (2.33)$$

A_{12} represents the mass transfer area for the transfer between

monomer phase and polymer phase. A_{34} represents the mass transfer area for the transfer between VCM droplet surface (skin) and aqueous phase. Similarly the areas A_{13},A_{45} are for the transfer between monomer phase and skin phase and between aqueous and vapor phase respectively.

N is the number of primary particles per unit volume of initial monomer and this quantity decreases with conversion. As the polymerization temperature increases, the size of the primary particles at a given conversion also increases [24]. At higher polymerization temperatures there are fewer primaries. At all polymerization temperatures the diameter of the primaries tends to the same limiting value at higher conversions, approximately 1.4μm. Above a conversion of 0.03, the particles flocculate to produce larger units. This flocculation process can be modelled by

$$N = N_{\infty} + (N_0 - N_{\infty})e^{-\xi x} \qquad (2.34)$$

Here the initial concentration N_0 is proportional to initiation rate and is determined mainly by temperature and nature/concentration of the initiator [28]. The final concentration N_{∞} has been found to vary with reaction temperature but it is around $2.5*10^{14}/dm^3$. The flocculation coefficient ξ is determined largely by the temperature of the process and the nature of the agitation. The coefficient ξ controls the rate of mass transfer of growing chains,monomer and initiator between monomer and polymer phase through the area A_{12}.

2.6 Energy Balance Equations

For the non isothermal polymerization of vinyl chloride in a batch reactor an overall energy balance around the reactor yields

the following dynamic equations.

The energy balance on cooling water in jacket coil is given below. Since coolant temperature rise is significant and flow is like plug flow inside the coil, an average jacket temperature T_{ja} may be used.

$$T_{ja} = \frac{T_{jai} + T_{jae}}{2}$$

where T_{jai} and T_{jae} are coolant inlet and exit temperatures respectively.

$$V_{ja}\,\rho_w\,C_w\,\frac{dT_{ja}}{dt} = \dot{m}_{ja}C_w(T_{jai} - T_{jae}) + h_{ja}A_{ja}(T_{m1} - T_{ja}) \qquad (2.35)$$

Similarly for energy balance on cooling water in baffles,

$$T_{bf} = \frac{T_{bfi} + T_{bfe}}{2}$$

where T_{bfi} and T_{bfe} are coolant inlet and exit temperatures respectively.

$$V_{bf}\,\rho_w\,C_w\,\frac{dT_{bf}}{dt} = \dot{m}_{bf}C_w(T_{bfi} - T_{bfe}) + h_{bf}A_{bf}(T_{m2} - T_{bf}) \qquad (2.36)$$

For metal wall energy balance, the temperature of the wall is treated as a lumped parameter.

$$V_{m1}\,\rho_{mw}C_m\,\frac{dT_{m1}}{dt} = h_{in}A_{ja}(T - T_{m1}) + h_{ja}A_{ja}(T_{m1} - T_{ja}) \qquad (2.37)$$

$$V_{m2}\,\rho_{mw}C_m\,\frac{dT_{m2}}{dt} = h_{in}A_{bf}(T - T_{m2}) + h_{bf}A_{bf}(T_{m2} - T_{bf}) \qquad (2.38)$$

where eqn (2.37) and eqn (2.38) are for the energy balance for jacket metal wall and baffle metal wall respectively.

For total reaction mass, perfect mixing and constant holdup and constant physical properties are assumed in the reactor. This gives the reactor energy balance as

$$V_R \rho_r C_p \frac{dT}{dt} = h_{in} A_{ja} (T - T_{m1}) + h_{in} A_{bf} (T - T_{m2}) + (-\Delta H) M_0 \frac{dx}{dt} + H_a \qquad (2.39)$$

where H_a is the heat developed by agitation.

2.7 Branching Characteristics

The nature and mechanism of formation of so-called anomalous structures in PVC have been the subject of extensive studies over the years. The progress made in understanding the nature of chain transfer to monomer and of the formation of anomalous structures in PVC is to a large extent due to the rapid development of new sensitive NMR techniques. The now accepted mechanism of chain transfer to the monomer has appeared in a recent paper by Hjertberg and Sorvik [29]. The reaction scheme is given in Fig 2.4a and Fig 2.4b.

According to this mechanism,the chain transfer to monomer starts with a head-to-head addition to the growing radical giving 2. This new radical can take part in a propagation reaction which results in the formation of internal head-to-head arrangements in the polymer. The radical 2 is very reactive and can stabilise itself by rearranging to 3. Propagation of this radical leads to the formation of chloromethyl side chain branching. The concentration of chloromethyl branches in technical PVC is about 4-5 per 1000 monomer units. By expulsion of chlorine radical 3 gives a polymer with a 1-chloro-2-alkene end group. The chain transfer to monomer is completed when the chlorine atom adds a

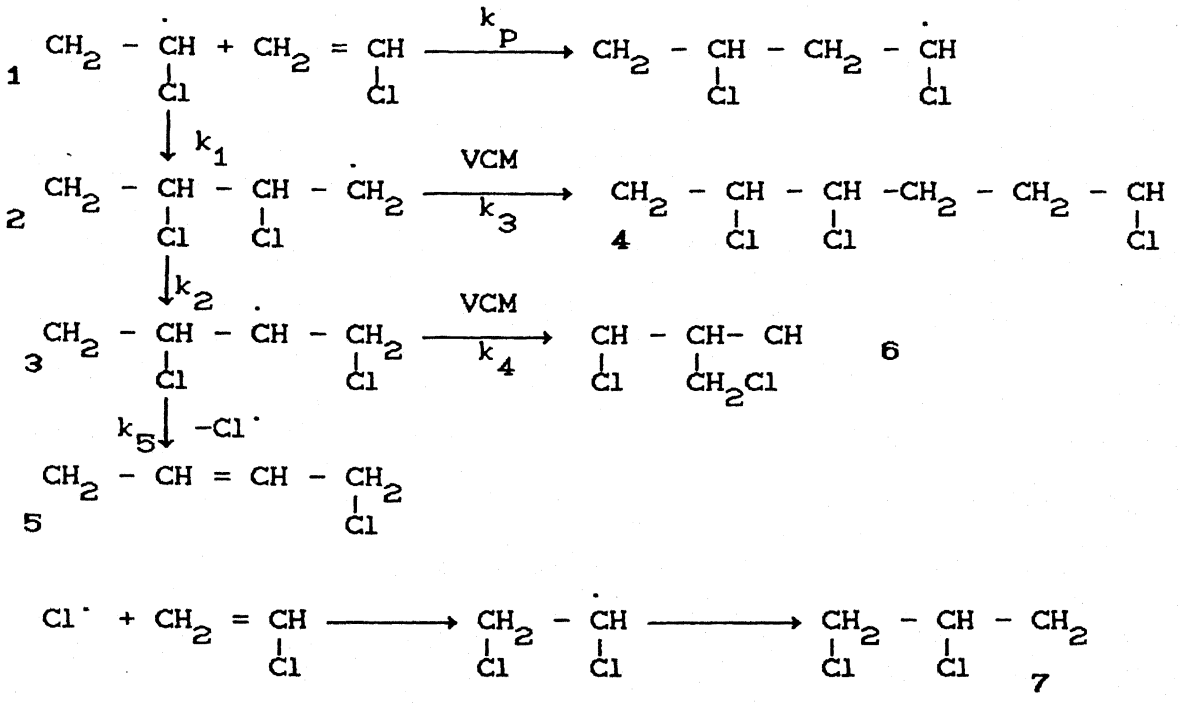

Fig 2.4a Reaction Scheme for chain transfer to monomer and for the formation of important anomalous structures in PVC

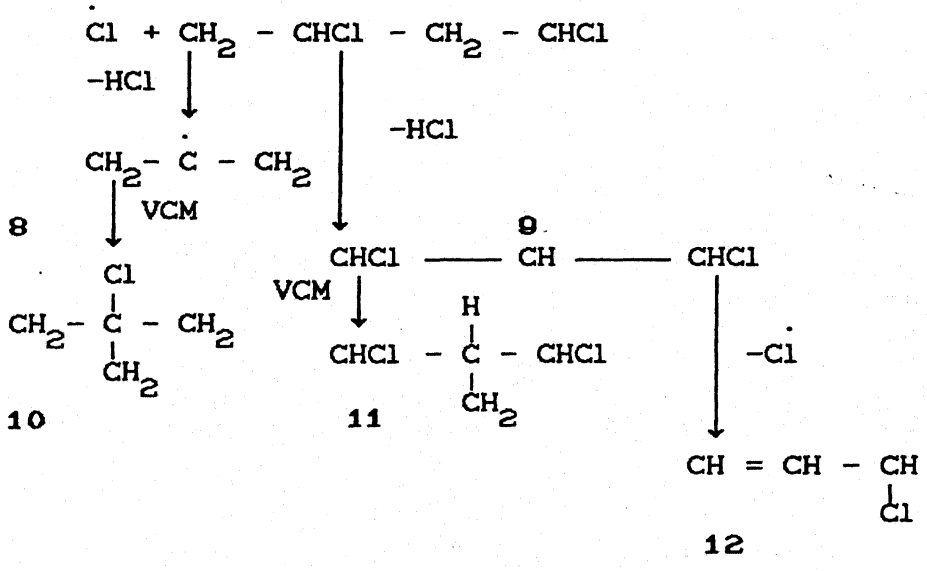

Fig 2.4b Reaction Scheme for chain transfer to polymer by chlorine atom and the formation of long chain branches and internal unsaturation in PVC

monomer unit and starts a new growing chain, which will have a 1,2 dichloro alkane end group (7). Structures 5 and 7 should be the most frequent end groups in PVC. In ordinary PVC, the content of these structures is somewhat less than one per molecule. The content of internal head-to-head arrangements in PVC is very low and not higher than 0.2 per 1000 monomer units.

Chlorine radicals can also take part in chain transfer to polymer. This is illustrated by the reaction scheme of Fig 2.4a. The first reaction in this scheme gives rise to the formation of one molecule of hydrochloric acid. Attack by the chlorine atom on the methylene group with subsequent expulsion of chlorine offers an explanation of the formation of internal unsaturation in PVC shown by structure 12. Propagation of intermediate radicals 8 and 9 leads to the formation of long chain branches (0.5 per 1000 monomer units). These propagation will give long chain branches associated with a tertiary chlorine (structure 10) or a tertiary hydrogen (structure 11). The attack by chlorine on the methylene group seems to be the preferred route.

Long chain branches in PVC may also arise by attack of a macroradical on the polymer. In this case the attack is primarily on the chloromethyl group, giving structure 8. Other anomalous structures in PVC can be found by backbiting. This gives 2,4-di chlorobutyl branches (about 1 per 1000 monomer units). The amount of both long and short chain branches increases as the monomer concentration in the polymer phase decreases.

In spite of progress made in explaining the formation of short and long chain branches in PVC, the now accepted mechanism of transfer to monomer and polymer are very difficult to

incorporate in a quantitative mathematical analysis of the polymerization due to the large number of unknown kinetic rate constants involved. In the present analysis it is assumed [14] that transfer to polymer and intramolecualr reactions are responsible for the formation of short and long chain branches respectively in PVC. This considerably simplifies the quantitative analysis of the polymerization since only two lumped rate constants k_{trp} and k_b need to be identified. Accordingly, L_n the average number of long branches per polymer chain and S_n the average number of short branches per chain can be obtained from the solutions of below equations,

$$\frac{d(\lambda_o L_n)}{dt} = M_o \left(k_{trp}/k_p\right) \left(\frac{x}{1-x}\right) \frac{dx}{dt} \qquad (2.40)$$

$$\frac{dS_n}{dt} = k_b \sigma_o \qquad (2.41)$$

The corresponding Long Chain Branches (LCB) and Short Chain Branches (SCB) per 1000 monomer units be given by

$$LCB = 1000 \left(L_n \lambda_0/\lambda_1\right) \qquad (2.42)$$

$$SCB = 1000 \left(S_n \lambda_0/\lambda_1\right) \qquad (2.43)$$

CHAPTER 3
OPTIMIZATION

3.1 Objective

The objective of the problem is to utilise the maximum cooling capacity of the reactor. This can be achieved by keeping the rate of polymerization uniform at the maximum rate possible. This is possible by adjusting the temperature during the process, according to an optimal temperature profile.

3.2 Single Objective Optimization

The single objective optimization technique is based on **Pontryagin's Continuous Minimum Principle.**

We can formulate the single objective optimization problem for

$$\text{Objective} \qquad \text{Min } I = \int_0^t F(\bar{y},\bar{u})\, dt \qquad (3.1)$$

subject to the following constraints

state equations : $$\frac{d\bar{y}}{dt} = \dot{\bar{y}} = \dot{\bar{f}} \qquad (3.2)$$

control variable constraints : $$\bar{u}_{min} < \bar{u} < \bar{u}_{max}$$

Let us assume there are n state variables and m control variables.

The **Hamiltonian** is set up as

$$H = F + \sum_{i=1}^{n} \lambda_i f_i \qquad (3.3)$$

λ's are time dependent **lagrange multipliers** (adjoint variables)

The adjoint variables are governed by

$$\frac{d\lambda_i}{dt} = -\frac{\partial H}{\partial y_i} \qquad i=1,2,\ldots\ldots\ldots,n \qquad (3.4)$$

Let time be floating and one of the state variable say y_k is fixed, then terminal conditions for the adjoint equations are calculated as follows,

$$\lambda_i(t_f) = 0.0 \qquad i=1,2,.....,(1-k) \qquad (3.5)$$

$$F + \lambda_k f_k = 0.0 \qquad (3.6)$$

$$\lambda_i(t_f) = 0.0 \qquad i=(k+1),.....n \qquad (3.7)$$

The control variables are then updated for $(j+1)^{th}$ iteration as follows,

$$u_i^{j+1} = u_i^j + \epsilon_i \frac{\partial H}{\partial u_i} \qquad \text{at any time t} \qquad (3.8)$$

$$i=1,2,.....,m$$

ϵ is a constant value which is computed using a simplex technique which minimizes the objective function.

3.3 Formulation for PVC Suspension Polymerization

For the present optimization studies we focus on keeping the rate profile flat.

$$\text{Min } I = \int_0^t (r_p - r_d)^2 \frac{dx}{dt}\, dt \qquad (a)$$

Comparing the above integrand with eqn (3.1)

$$F = (r_p - r_d)^2 \frac{dx}{dt} \qquad (b) \qquad (3.9)$$

where r_p is the rate predicted and r_d is the desired rate of polymerization. In this case time is floating and terminal conversion is fixed. Reaction mass temperature is the control variable.

$\bar{u} = T$ total number of control variables $m = 1$

The state variables are represented by

$$\bar{y} = (I_1, I_2, I_3, M_1, M_2, M_3, M_4, M_5, \sigma_{01}, \sigma_{02}, \sigma_{03}, \sigma_{11}, \sigma_{12}, \sigma_{13}, \sigma_{21}, \sigma_{22},$$
$$\sigma_{23}, \lambda_{02}, \lambda_{03}, \lambda_{12}, \lambda_{13}, \lambda_{22}, \lambda_{23}, V_1, V_2, V_3, V_4, V_5, x, (L_n\lambda_0), S_n)^T$$

(3.10)

Total number of state variables n = 31

The state equations are given in Table 3.1

control variable constraints : $T_{min} < T < T_{max}$

The commercial reactor operating temperature ranges from 40°C to 75°C.

The above state equations are solved by forward integration with suitable initial value for each variable.

The **Hamiltonian** is set up as

$$H = F + \sum_{i=1}^{31} \lambda_i f_i \qquad (3.11)$$

The adjoint equations are given as,

$$\frac{d\lambda_i}{dt} = - \frac{\partial H}{\partial y_i} \qquad i=1,2,3,.....,31 \qquad (3.12)$$

The terminal conditions are

$$\lambda_i(t_f) = 0.0 \qquad i=1.2,.....,28 \qquad (3.13)$$

$$F + \lambda_{29} f_{29} = 0.0 \qquad (3.14)$$

$$\lambda_i(t_f) = 0.0 \qquad i=30,31 \qquad (3.15)$$

Integrate the adjoint equations backward. Update the control variable as follows,

$$T^{j+1} = T^j + \varepsilon \frac{\partial H}{\partial T} \qquad \text{at any time t} \qquad (3.16)$$

Repeat the procedure from the starting point till convergence is achieved. The flow chart for this single objective optimization problem is given in Fig 3.1

Table 3.1 State Equations for the Optimization Problem

The state equations are given as,

$\frac{dy}{dt}_j = \frac{dI}{dt}_i = f_j$	i=1,2,3	j=1,2,3
$\frac{dy}{dt}_j = \frac{dM}{dt}_i = f_j$	i=1,2,...,5	j=4,5,...,8
$\frac{dy}{dt}_j = \frac{d\sigma}{dt}_{0i} = f_j$	i=1,2,3	j=9,10,11
$\frac{dy}{dt}_j = \frac{d\sigma}{dt}_{1i} = f_j$	i=1,2,3	j=12,13,14
$\frac{dy}{dt}_j = \frac{d\sigma}{dt}_{2i} = f_j$	i=1,2,3	j=15,16,17
$\frac{dy}{dt}_j = \frac{d\lambda}{dt}_{0i} = f_j$	i=2,3	j=18,19
$\frac{dy}{dt}_j = \frac{d\lambda}{dt}_{1i} = f_j$	i=2,3	j=20,21
$\frac{dy}{dt}_j = \frac{d\lambda}{dt}_{2i} = f_j$	i=2,3	j=22,23
$\frac{dy}{dt}_j = \frac{dV}{dt}_i = f_j$	i=1,2,...,5	j=24,.....,28
$\frac{dy}{dt}_j = \frac{dx}{dt} = f_j$		j=29
$\frac{dy}{dt}_j = \frac{d(\lambda_0 L_n)}{dt} = f_j$		j=30
$\frac{dy}{dt}_j = \frac{dS}{dt}_n = f_j$		j=31

Fig 3.1 Flow chart for the single objective optimization probelm

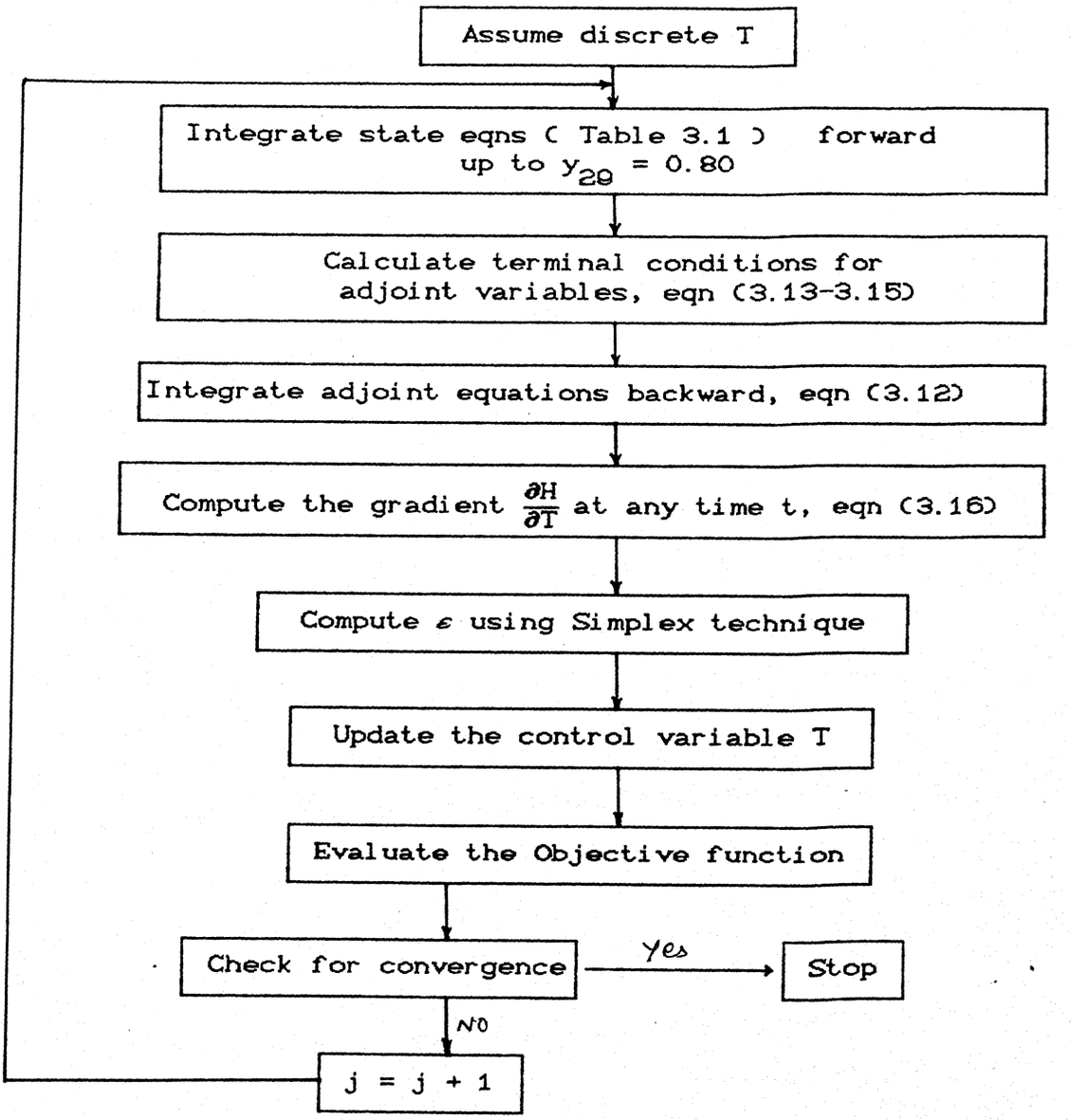

CHAPTER 4
RESULTS AND DISCUSSIONS

In the first section of our discussion in this chapter we analyse the model prediction. In the second section we have used our model to optimize the reactor performance using the formulation in Chapter 3. And in the last section we have used the energy balance equations reorganised in Appendix II to estimate the various heat transfer coefficients.

4.1 Simulation Results of the Model

The system of coupled ordinary differential equations (2.8-2.19, 2.40, 2.41) have been solved numerically by the Gear algorithm (using NAG routine D02EBF) on HP 9000 computer.

It is assumed that there is no initiator available in water and vapor phases. Though it is true that little polymerization [19] does take place in water phase, in this present analysis it is assumed that there will be no polymerization in water as well as vapor phase also. It is also assumed that there is no transfer of initiator and radicals between skin and other phases. Monomer in water and vapor phases, though not involved in any reaction, is exchanged between these two phases and the other neighbouring phases. Moreover, the transfer of monomer to polymer phase from vapor phase after the critical conversion is important since it is accompanied by a pressure drop in the reactor. It is assumed that there is no dead polymer in monomer phase. As soon as radical gets terminated in the monomer phase, it precipitates out into the polymer and skin phases.

The simulation is done under non isothermal condition. We used the reactor temperature profile reported by industry for our

simulation purpose. In this present work momomer charge is added in one slot i.e., $F_M = 0.0$.

Effect of Kinetic Rate Constants

The various rate constants used for simulation in our study have been reported in chapter 2. For the skin phase the rate constants have been taken as same in polymer phase. The initiator efficiency factor f_2 in polymer phase and f_3 in skin phase are taken as same where as f_1 in monomer phase is much higher than that in other phases. Although Hamielec [10] has reported that kinetic behaviour of suspension PVC would change after critical conversion when we used his kinetic rate constants for our model we did not obtain acceptable results. The polymerization rate decreased drastically consequently it took long time to increase conversion. The result of this work is shown in Fig 4.1. Xie [11] has used his equations and found that Hamielec modelling attempts were premature due to the inadequate amount of kinetic data at these high conversion levels.

Diffusivities and Mass Transfer Coefficients

The necessary data related to mass transfer of species between the various phases (including the partition coefficients) are reported in Table 4.1. Diffusivities D^I_{12}, D^M_{13}, D^M_{34}, D^M_{45} are estimated using standard correlations which have been referred to in [27]. D^M_{12} is obtained from reference [18]. The non - fickian diffusion effect of D^M_{12} has been quantised and found to be one order less than that of fickian diffusion value. In that range we conducted sensitivity analysis and found it was insensitive to both polymerization rate and pressure profile. The calculation of non - fickian diffusivity is shown in Appendix III.

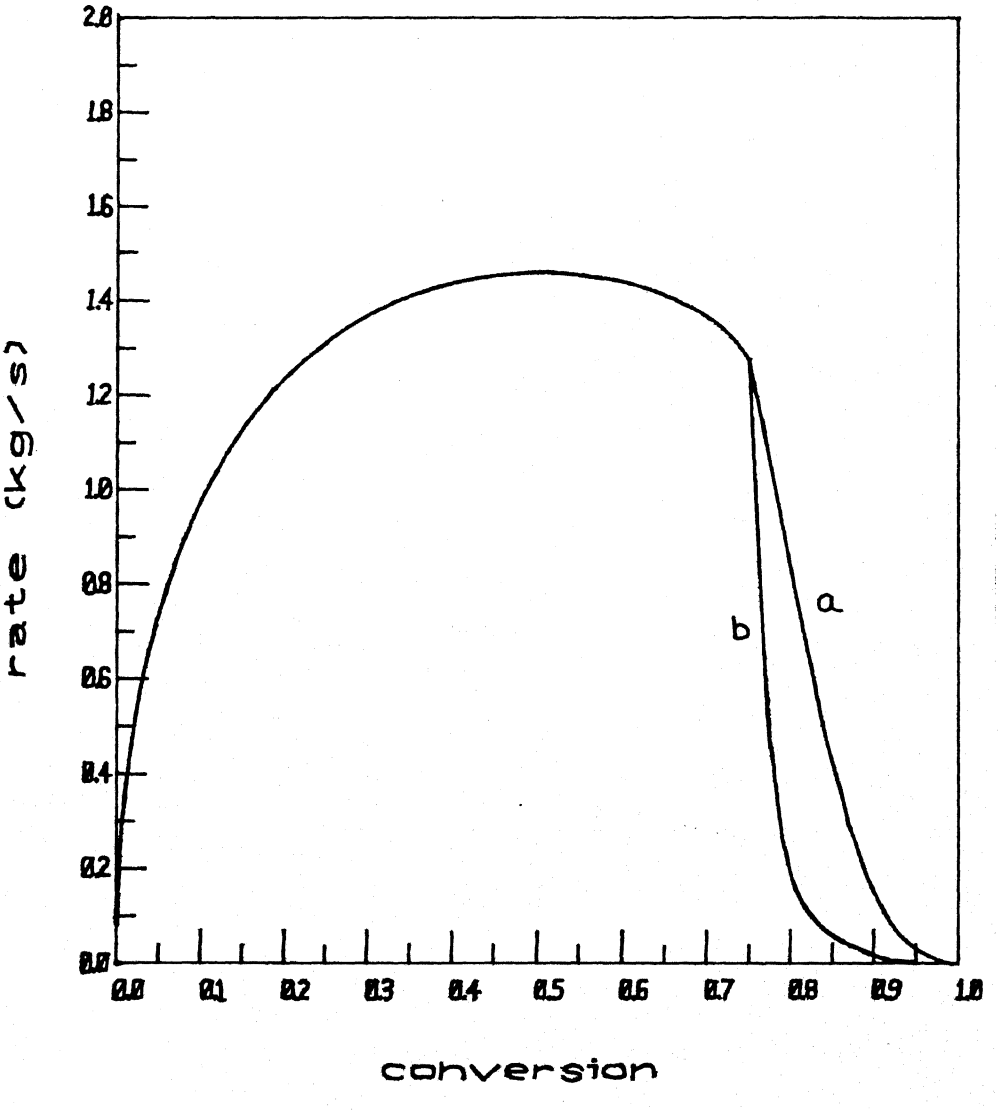

Fig 4.1 Effect of rate constants

a) Sidiropolou rate constants

b) Hamielec rate constants

Table 4.1

Necessary Data for Mass Transfer of Species Between Various Phases and Partition Coefficients

			Ref
1. Diffusivities			
a.	$D^{I}_{12} = 6.1398 \times 10^{14}$	dm^2/sec	[27]
b.	$D^{M}_{12} = 2.0 \times 10^{-13}$	dm^2/sec	[27]
c.	$D^{M}_{34} = D^{M}_{13} = 4.435 \times 10^{-8}$	dm^2/sec	[27]
d.	$D^{M}_{45} = 5.4903 \times 10^{-8}$	dm^2/sec	[27]
e.	$D^{R}_{12} = 10^{-5} - 10^{-14}$	dm^2/sec	[7]
2. Mass transfer areas			
a.	$A_{12} = A_{21} = [36\ \pi\ N\ V_0 V_2]^{1/3}$	dm^2	[7]
b.	$A_{13} = A_{31} = A_{34} = A_{43}$ based on droplet dia of 50μm and total droplet number 4×10^{14}	dm^2	[7]
c.	$A_{45} = A_{54} = 1140.09$	dm^2	[7]
3. Mass transfer coefficients			
a.	$k^{I}_{M12} = D^{I}_{12} R_p^{-1} = D^{I}_{12} \left[\frac{4\ \pi\ N\ V_0}{3V_2}\right]^{1/3}$	dm/sec	[7]
b.	$k^{M}_{M12} = D^{M}_{12} \left[\frac{4\ \pi\ N\ V_0}{3V_2}\right]^{1/3}$	dm/sec	[7]
c.	$k^{R}_{M12} = D^{R}_{12} \left[\frac{4\ \pi\ N\ V_0}{3V_2}\right]^{1/3}$	dm/sec	[7]
d.	$k^{M}_{M13} = k^{M}_{M34} = 1.774 \times 10^{-4}$	dm/sec	[27]
e.	$k^{M}_{M45} = 1.000 \times 10^{-4}$	dm/sec	
f.	$k^{y}_{Mji} = \gamma^{y}_{ij}\ k^{y}_{Mij}$		[27]

4. Partition Coefficients

a.	γ_{12}^{M}	=	3.0 - 5.0	
b.	γ_{13}^{M}	=	3.04	[27]
c.	γ_{34}^{M}	=	23.59	[27]
d.	γ_{45}^{M}	=	0.58	[27]
e.	γ_{12}^{R}	=	0.0001	[27]
f.	γ_{12}^{I}	=	1.0 - 20.0	[7]

The mass transfer coefficients reported in Table 4.1 are obtained from the relationship Sh = 2.0, except the mass transfer coefficient k_{45}^{M}. This mass transfer coefficient is found to be very sensitive to pressure drop in the reactor which is discussed later in detail. Correlations of Ranz-Marshall, Calderbank-Jones, Brian-Hales and Sh = 2.0 have been used [27] to calculate the mass transfer coefficients. Although the mass transfer coefficients calculated by different correlations are different the rate of polymerization and pressure have been found to be insensitive to these coefficients in that domain.

Partition Coefficients

The partition coefficients have been reported in Table 4.1. Among these partition coefficients, γ_{12}^{M} and γ_{12}^{I} have been found to be sensitive to polymerization rate, this is discussed later in detail.

As noted in section 2.2.1, at conversions less than 0.001, the polymerization takes place only in monomer rich phase. So, up to 0.001 conversion only monomer phase equations are simulated and after that the entire model is included. The skin phase is assumed to be formed at 0.001 conversion with the initial thickness of 0.1μm i.e., a mono particle layer of polymer [19].

The physical parameters used for simulation has been reported in Table 4.2.

Sensitivity Analysis

The effect of various model parameters on rate of polymerization and pressure have been studied to find out which parameters are more sensitive.

Table 4.2

Physical Parameters Used in Simulation

Parameters		Values	Units	Ref
1.	A_{bf}/A_{ja}	0.28940		[31]
2.	C_p	3.32	J/gm.K	[27]
3.	C_M	0.48	J/gm.K	[27]
4.	C_W	4.18	J/gm.K	[27]
5.	V_{m1}/V_R	0.0171		[31]
6.	V_{m2}/V_R	$2.0*10^{-3}$		[31]
7.	V_{bf}/V_R	0.01427		[31]
8.	V_{ja}/V_R	0.0312		[31]
9.	ρ_m	840.2	gm/dm^3	[9]
10.	ρ_p	1379.3	gm/dm^3	[9]
11.	ρ_{mw}	7850.0	gm/dm^3	[27]
12.	ρ_w	985.44	gm/dm^3	[9]
13.	MW_M	62.45	gm/gmole	[9]
14.	MW_I	346.45	gm/gmole	[31]
15	H/D_R	1.2934		[31]

The objective function for this sensitivity analysis has been formulated as follows,

$$I_1 = \int_0^t (r_p - r_d)^{2.0}\, dt \quad ; \quad I_2 = \int_0^t (p_p - p_d)^{2.0}\, dt$$

where I_1 and I_2 are the integral errors in polymerization rate and pressure respectively; r_p and r_d are the polymerization rate predicted by simulation and reference rate profile. Similarly p_p and p_d are the pressure predicted by simulation and reference pressure profile.

For each parameter lower and upper bound values have been found out by simulation experience. With these lower and upper bound values for each parameter, the polymerization rate and pressure have been simulated and the integral error I_1 and I_2 are calculated.

The various model parameters like kinetic parameter β, diffusivities D_{12}^R, mass transfer coefficients k_{M13M}^M, k_{M34M}^M, k_{M45M}^M and partition coefficients γ_{12}^I, γ_{12}^M, γ_{13}^M, γ_{34}^M, γ_{45}^M, γ_{12}^R have been taken for this analysis. We found among these parameters, γ_{12}^M, γ_{12}^I, D_{12}^R, and β are more sensitive to polymerization rate (in the same order as indicated) but insensitive to pressure profile. On the other hand k_{M45}^M has been found to be sensitive to pressure profile but insensitive to polymerization rate. All other parameters are neither sensitive to polymerization rate nor to pressure profile.

Effect of γ_{12}^M

The monomer partition coefficient between phase 1 and phase 2, γ_{12}^M is the most sensitive parameter to rate of

polymerization. A slight increase in the monomer concentration of polymer phase is enough to accelerate the reaction .The monomer concentration in the polymer phase is very important in determining the rate curve. The rate decreases drastically with increase in the value of γ_{12}^{M}. The effect of this on rate is shown in Fig 4.2. Since monomer phase disappears after critical conversion (x_c= 75%) the monomer in the polymer phase starts depleting thereby producing a steep fall in rate.

Effect of γ_{12}^{I}

As γ_{12}^{I} increases the rate of polymerization decreases. If γ_{12}^{I} is high then less amount of initiator is located in the polymer phase, therefore rate decreases where as for low value the initiator concentration in polymer phase is high so rate increases. Although the rate profile does vary with different γ_{12}^{I} values, it is not very significant. The reason for this is the initiator location is irrelevant for high radical diffusivity (D_{12}^{R} = 2.0*10^{-6} dm^2/sec). The effect of γ_{12}^{I} is shown in Fig 4.3.

Effect of D_{12}^{R}

The rate of radical mass transfer is crucial in determining the shape of the reaction rate profile. For a high value of D_{12}^{R}, in the range 10^{-5} - 10^{-8} radicals initiated in the monomer phase 1 diffuse rapidly into the polymer phase 2 and so essentially all growth takes place in phase 2. On the other hand for low radical diffusivity (D_{12}^{R} in the range 10^{-10} - 10^{-14} dm^2/sec) essentially there is no radical transfer, thus the rate peak is lowered. The effect of D_{12}^{R} on polymerization rate at different values is shown in Fig 4.4. We found that D_{12}^{R} has negligible effect on rate of polymerization in the range 10^{-5} - 10^{-8}. But in

the range 10^{-8} - 10^{-14} the rate profile decreases with decrease in D_{12}^{R}.

Effect of Initiator Efficiency Ratio ,β

The increase in initiator efficiency ratio has been found to increase the polymerization rate. As β increases more amount of initiator in the polymer phase decomposes to yield more radicals which triggers the polymerization reaction. This effect on rate is shown in Fig 4.5.

Effect of k_{M45}^{M}

The monomer interphase mass transfer coefficient between aqueous and vapor phase plays a vital role in determining the pressure drop in the reactor. If k_{M45}^{M} is very low then transfer of monomer into vapor phase is negligible thereby causing pressure to drop faster. On the other hand if it is high more amount goes into vapor phase reducing the pressure drop. Fig 4.6 shows the effect of k_{M45}^{M} on pressure profile.

Parameter Estimation

The objective function for parameter estimation has been formulated as follows,

$$\text{Min} \quad I_1 = \sum_{i=1}^{t_f} (r_p - r_d)^{2.0}$$

where r_p and r_d are the average rate of polymerization predicted by simulation and average rate of polymerization given by industry at every hour (up to t_f^{th} hour).

With initial estimates (Table 4.3) for the rate sensitive parameters the rate of polymerization is simulated and averaged over every hour. With this the error I_1 is calculated. The

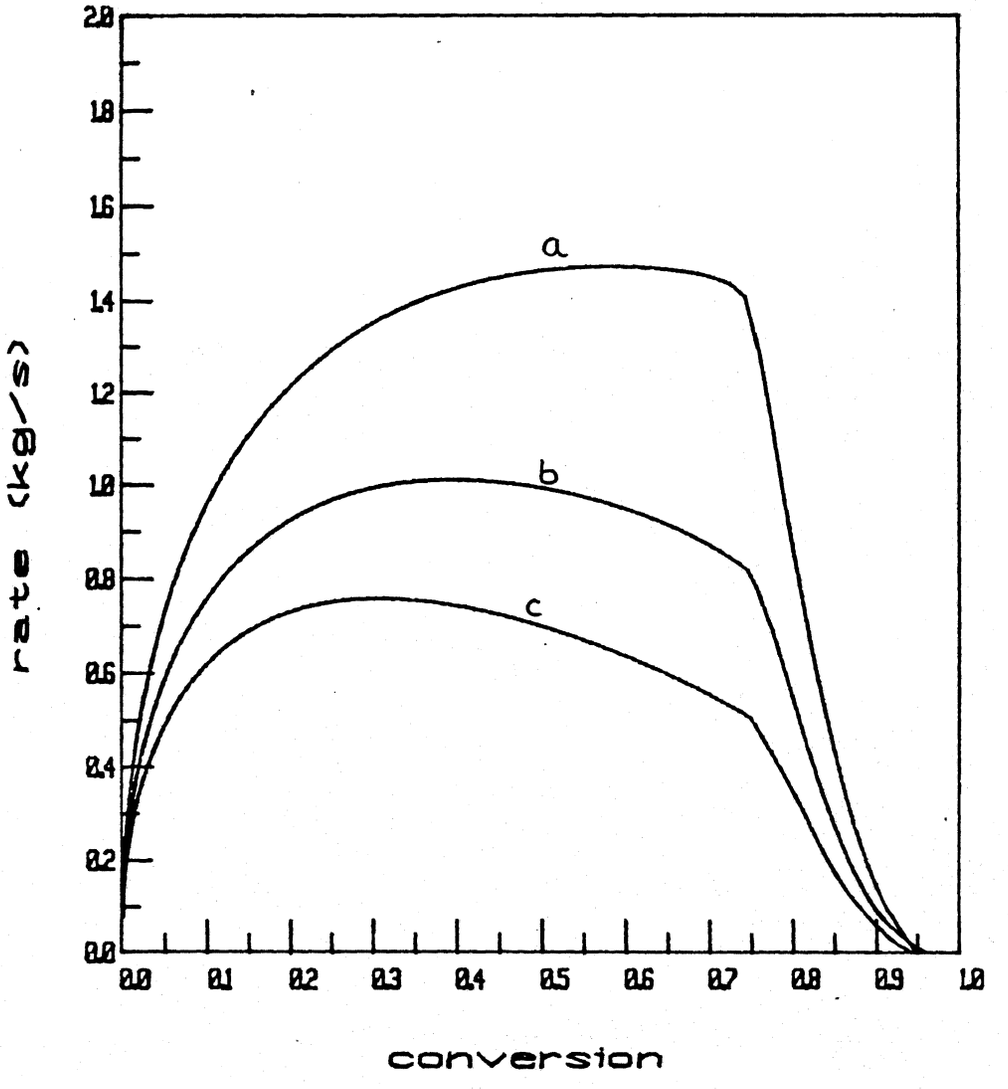

Fig 4.2 Effect of monomer partition coefficient γ_{12}^{M}

a) $\gamma_{12}^{M} = 3.0$; b) $\gamma_{12}^{M} = 3.5$; c) $\gamma_{12}^{M} = 4.0$

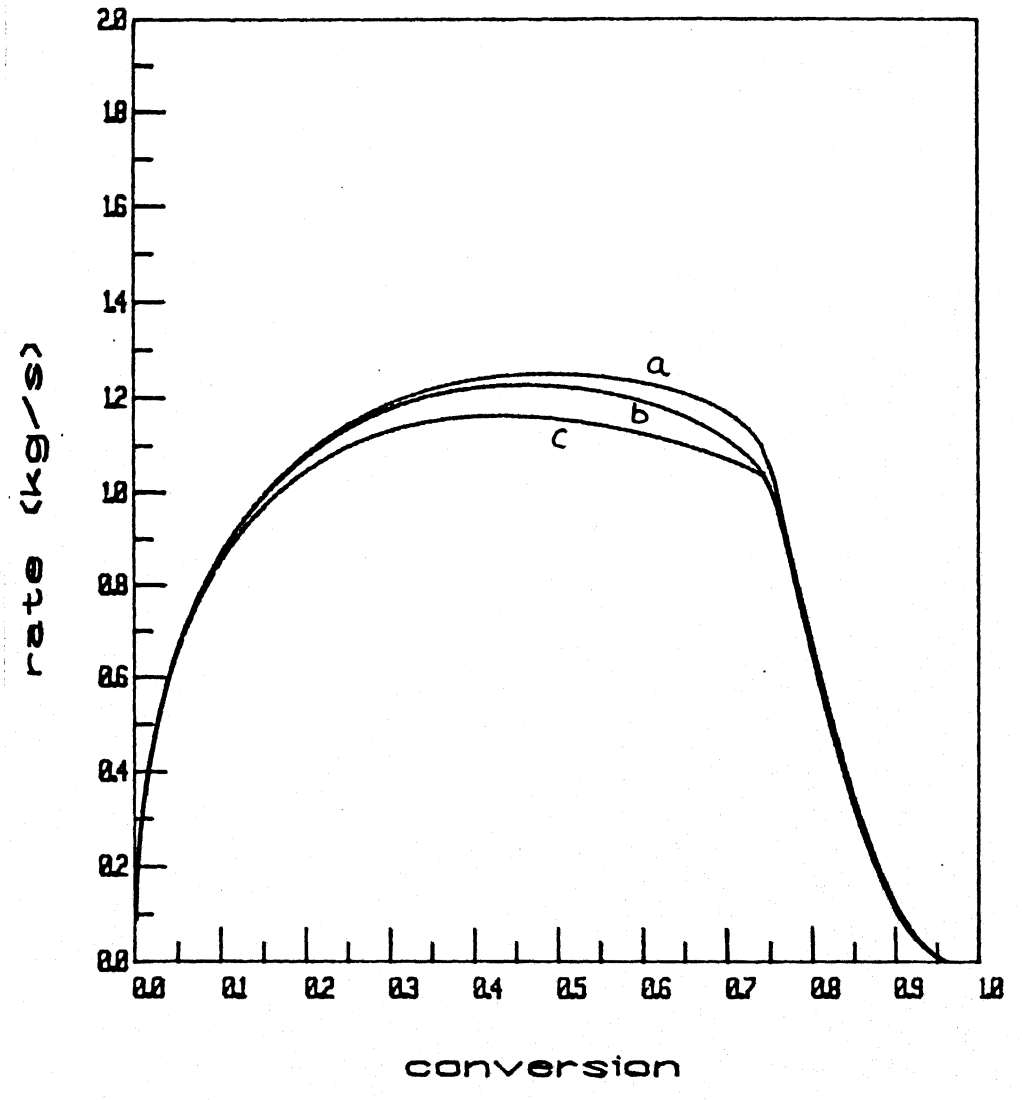

Fig 4.3 Effect of initiator partition coefficient γ_{12}^{I}

a) γ_{12}^{I} = 1.0 ; b) γ_{12}^{I} = 5.0 ; c) γ_{12}^{I} = 20.0

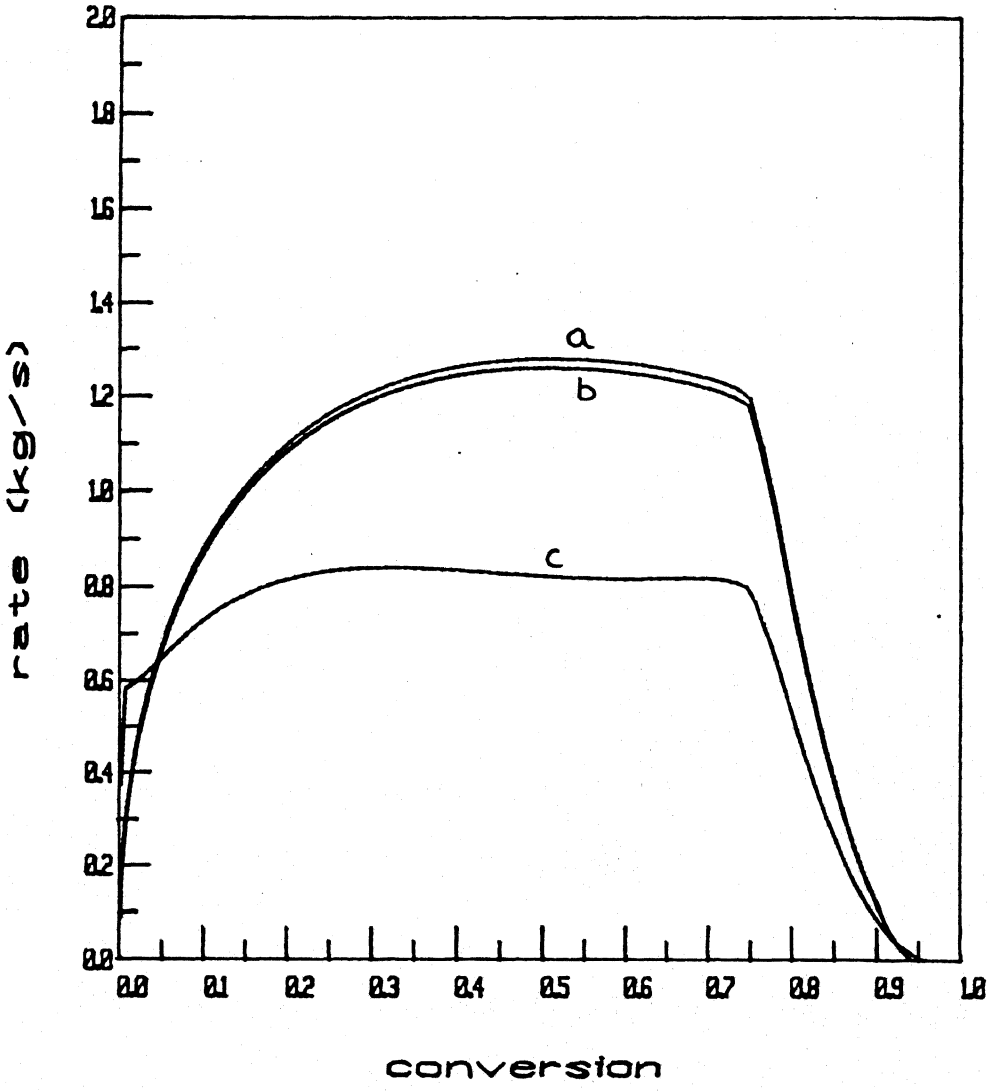

Fig 4.4 Effect of radical diffusivity D_{12}^{R}

a) $D_{12}^{R} = 1.0*10^{-6}$; b) $D_{12}^{R} = 1.0*10^{-8}$; c) $D_{12}^{R} = 1.0*10^{-11}$

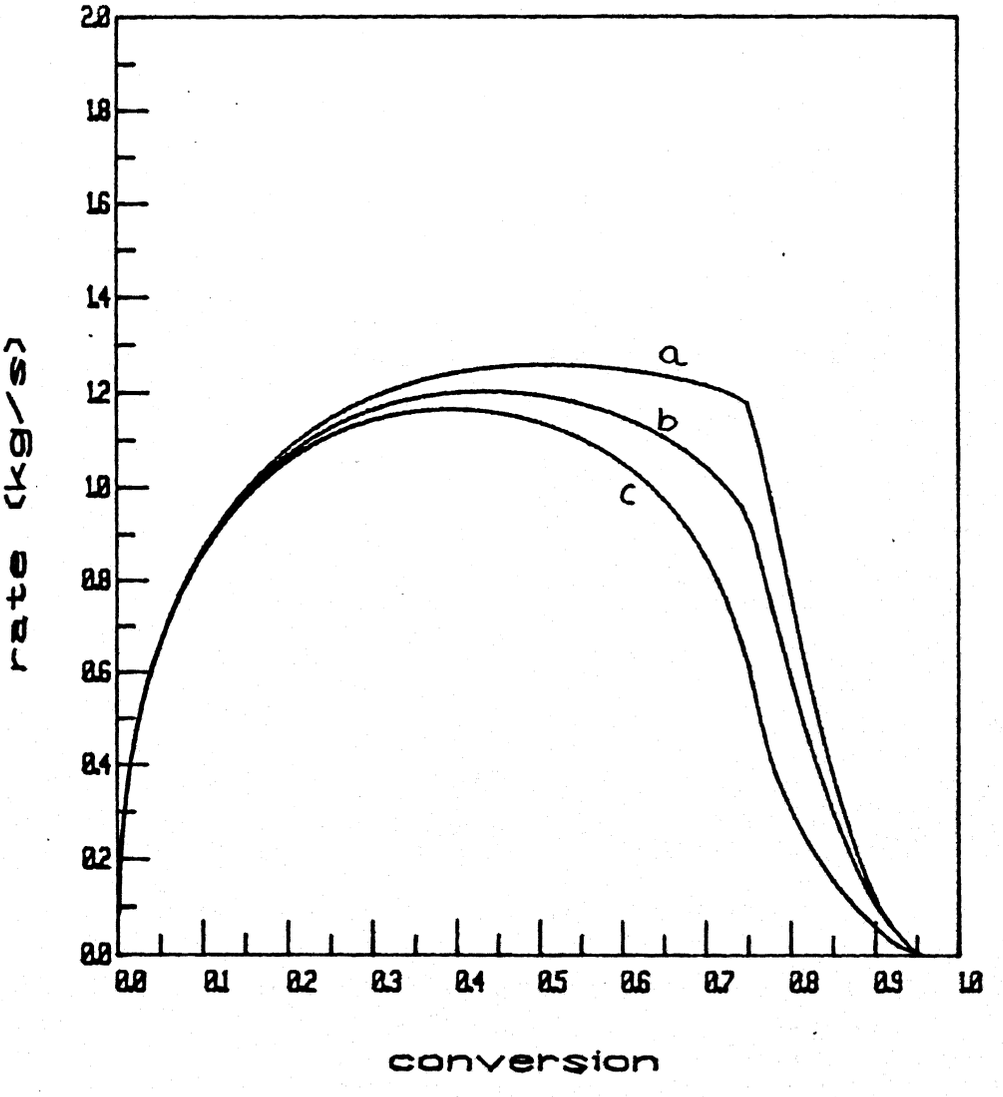

Fig 4.5 Effect of initiator efficiency ratio β

a) $\beta = 1.0$; b) $\beta = 0.5$; c) $\beta = 0.1$

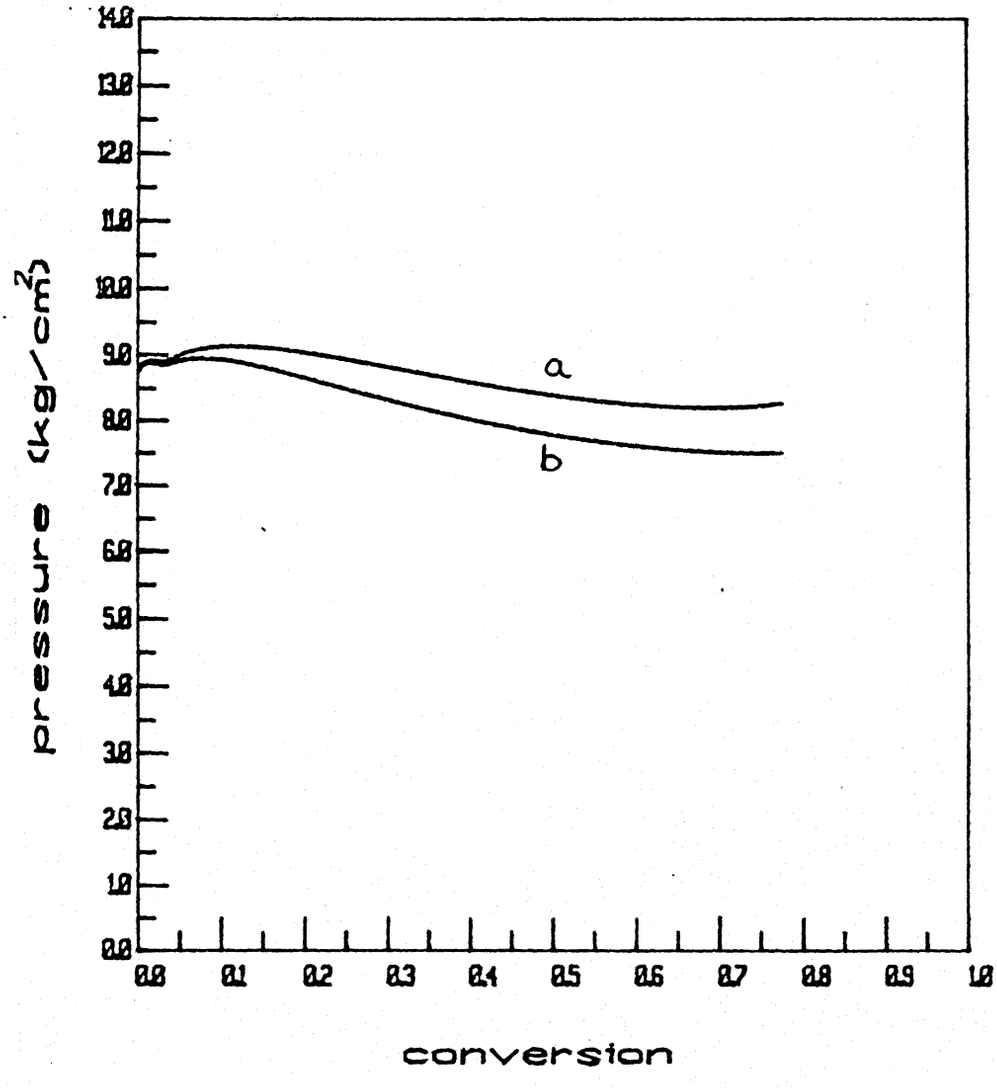

Fig 4.6 Effect of monomer interphase mass transfer coefficient k^{M}_{M45}

a) $k^{M}_{M45} = 1.0 \times 10^{-5}$; b) $k^{M}_{M45} = 1.0 \times 10^{-11}$

Table 4.3 Model parameter values used before and after parameter tuning

Parameters	Before Tuning	After Tuning	Ref
D_{12}^{I}	$6.1398*10^{14}$	$6.1398*10^{14}$	[27]
D_{12}^{M}	$2.0*10^{-13}$	$2.0*10^{-13}$	[27]
D_{34}^{M}	$4.435*10^{-8}$	$4.435*10^{-8}$	[27]
D_{45}^{M}	$5.4903*10^{-8}$	$5.4903*10^{-8}$	[27]
D_{13}^{M}	$4.435*10^{-8}$	$4.435*10^{-8}$	[27]
D_{12}^{R}	$1.0*10^{-7}$	$2.0*10^{-6}$	
γ_{12}^{M}	3.1	3.21	
γ_{13}^{M}	3.04	3.04	[27]
γ_{34}^{M}	23.59	23.59	[27]
γ_{45}^{M}	0.58	0.58	[27]
γ_{12}^{I}	3.448	3.7821	
γ_{12}^{R}	0.0001	0.0001	[27]
β	0.5	0.65	
k_{M45}^{M}	$1.0*10^{-4}$	$1.707*10^{-6}$	

parameters are then tuned, to minimize I_1, using simplex optimization technique.

Similarly pressure sensitive parameters are tuned to match simulated pressure with industrial pressure data.

The parameter estimation has been done for seven industrial runs. In all the runs the parameter values turn out to be nearly same, allowing us to take an average value for each parameter. The parameter values for seven runs is given in Table 4.4

With the estimated parameters the results are simulated. These results like rate of polymerization, pressure drop in the reactor, and conversion history matches well with industrial data. The comparison of industrial and our simulated conversion history, polymerization rate and pressure profile are shown in Fig 4.7a, Fig 4.8a, and Fig 4.9a. For second run the respective results are shown in Fig 4.7b, Fig 4.8b and Fig 4.9b.

4.2 Optimization Results

The system of coupled ODE's (Table 3.1) have been solved using NAG routine D02EBF. The derivative $\frac{\partial H}{\partial t}$ in equation (3.16) has been obtained numerically using NAG routine D04AAF. Again the system of coupled ODE's equation (3.12) has been solved using D02EBF routine. The weighting factor ε has been calculated using simplex technique E04CCF in NAG.

First with the initially assumed temperature profile to be flat at 330K the equations in Table 3.1 have been solved to get the state variable values. These equations are solved till conversion reaches 80%. The reason for choosing terminal conversion as 80% is above this conversion it is not possible to keep the rate profile flat as there is virtually no monomer in

Table 4.4 Parameter Estimation For Seven Runs

Runs	γ_{12}^{M}	γ_{12}^{I}	D_{12}^{R}	β	k_{M45M}^{M}
1.	3.1965	4.038	2.982×10^{-6}	0.65	1.70×10^{-6}
2.	3.2160	3.4073	1.491×10^{-6}	0.64	1.70×10^{-6}
3.	3.1900	3.804	5.600×10^{-6}	0.642	1.70×10^{-6}
4.	3.2080	3.502	2.000×10^{-6}	0.65	1.70×10^{-6}
5.	3.1916	4.278	8.000×10^{-7}	0.646	1.70×10^{-6}
6.	3.2201	4.028	2.689×10^{-6}	0.649	1.70×10^{-6}
7.	3.2143	3.4167	5.999×10^{-7}	0.653	1.70×10^{-6}

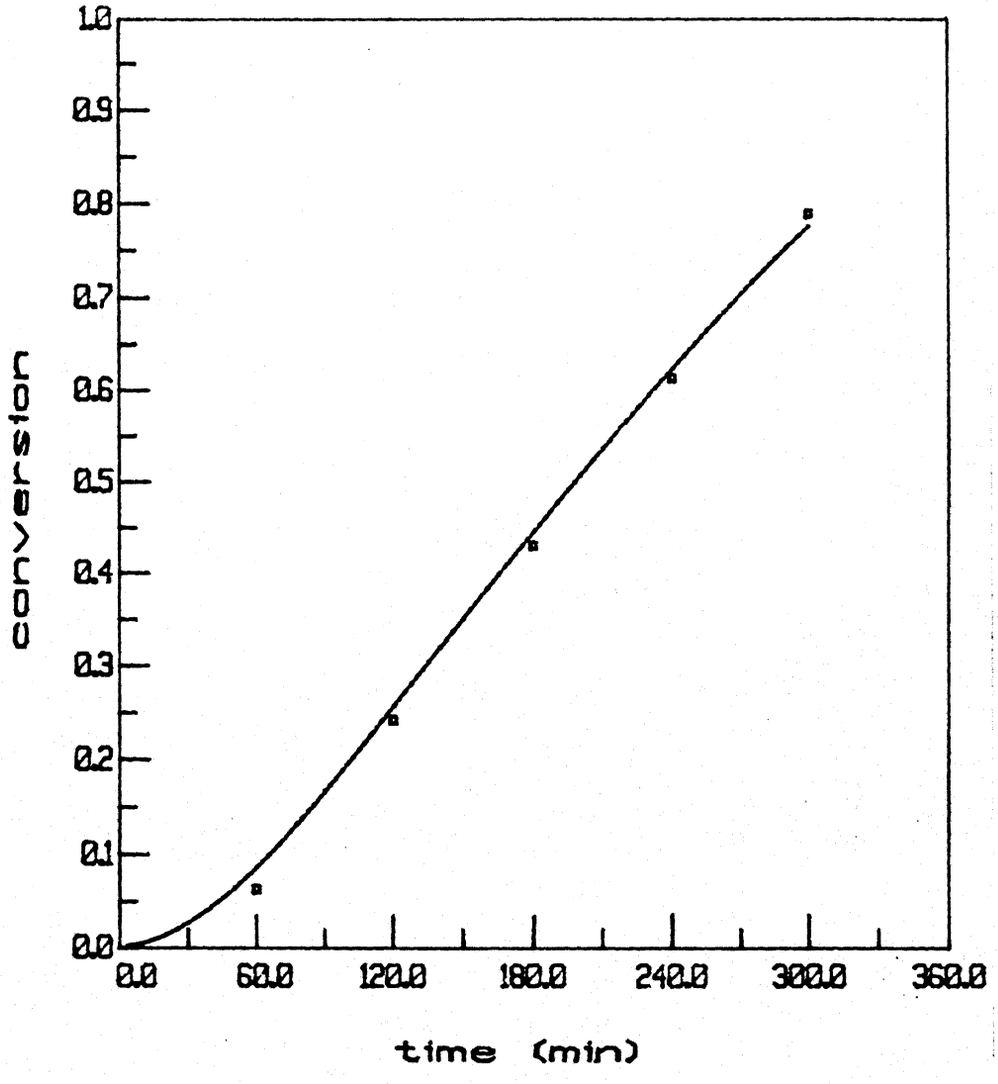

Fig 4.7a Comparison of conversion history between experimental data and model prediction for run 1

▫, experimental data ; —— model

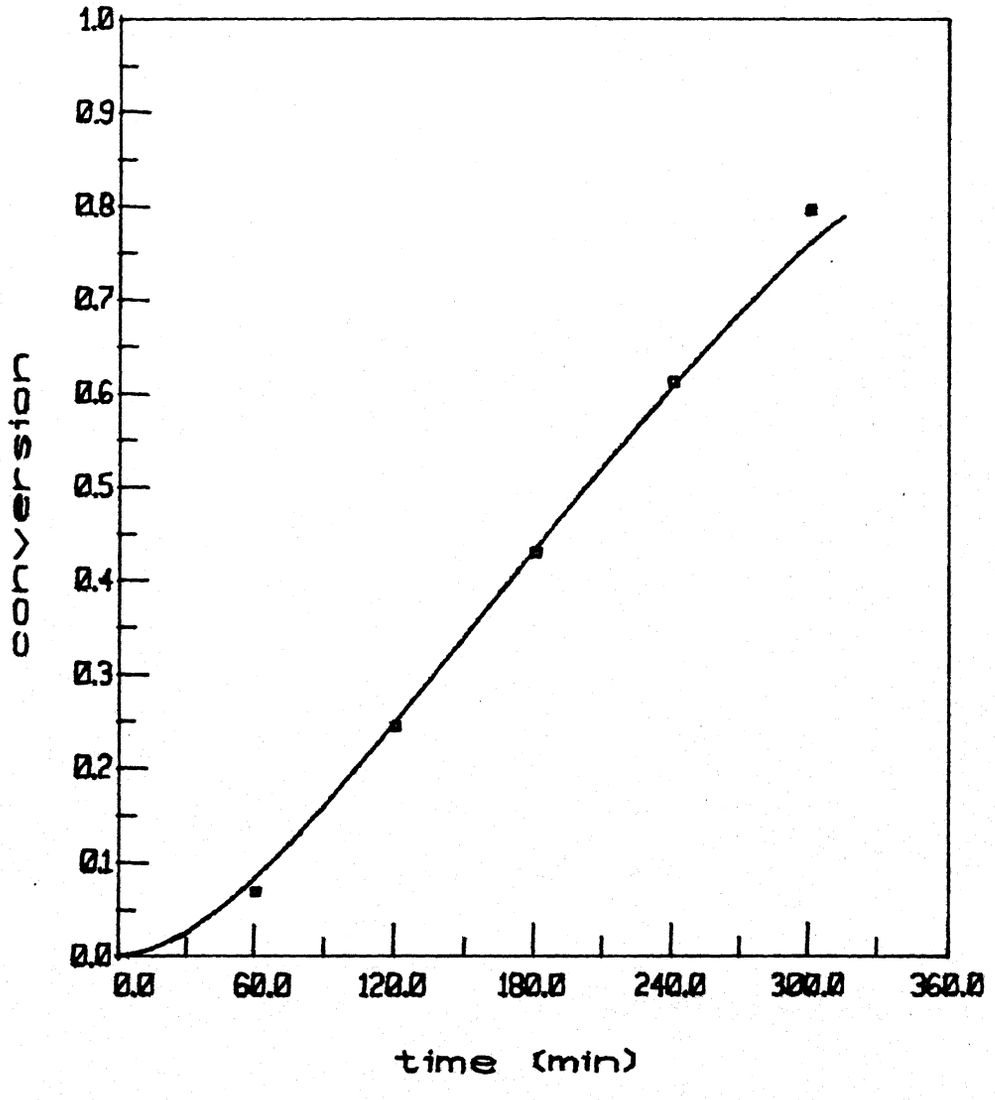

Fig 4.7b Comparison of conversion history between experimental data and model prediction for run 2

▫, experimental data ; —— model

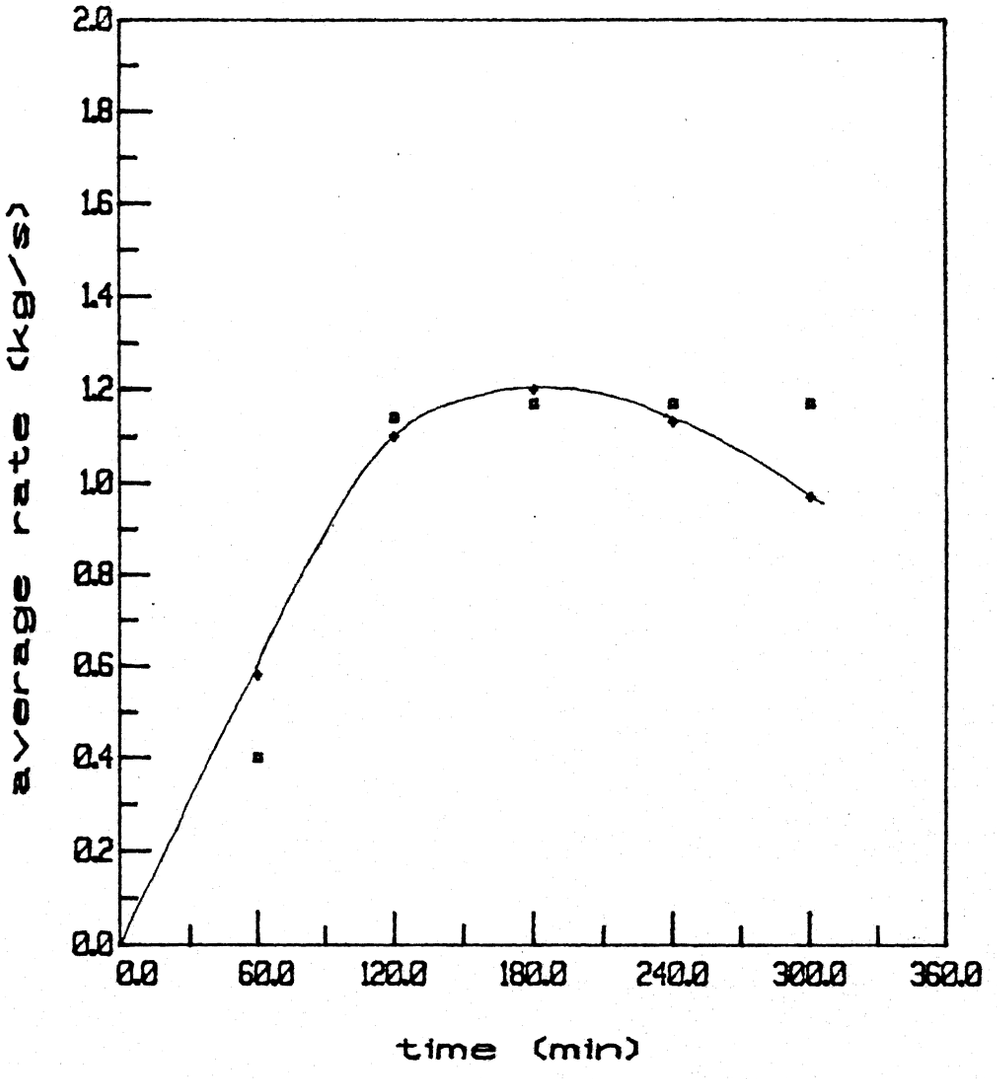

Fig 4.8a Comparison of polymerization rate between experimental data and model prediction for run 1

□, experimental data ; —— model

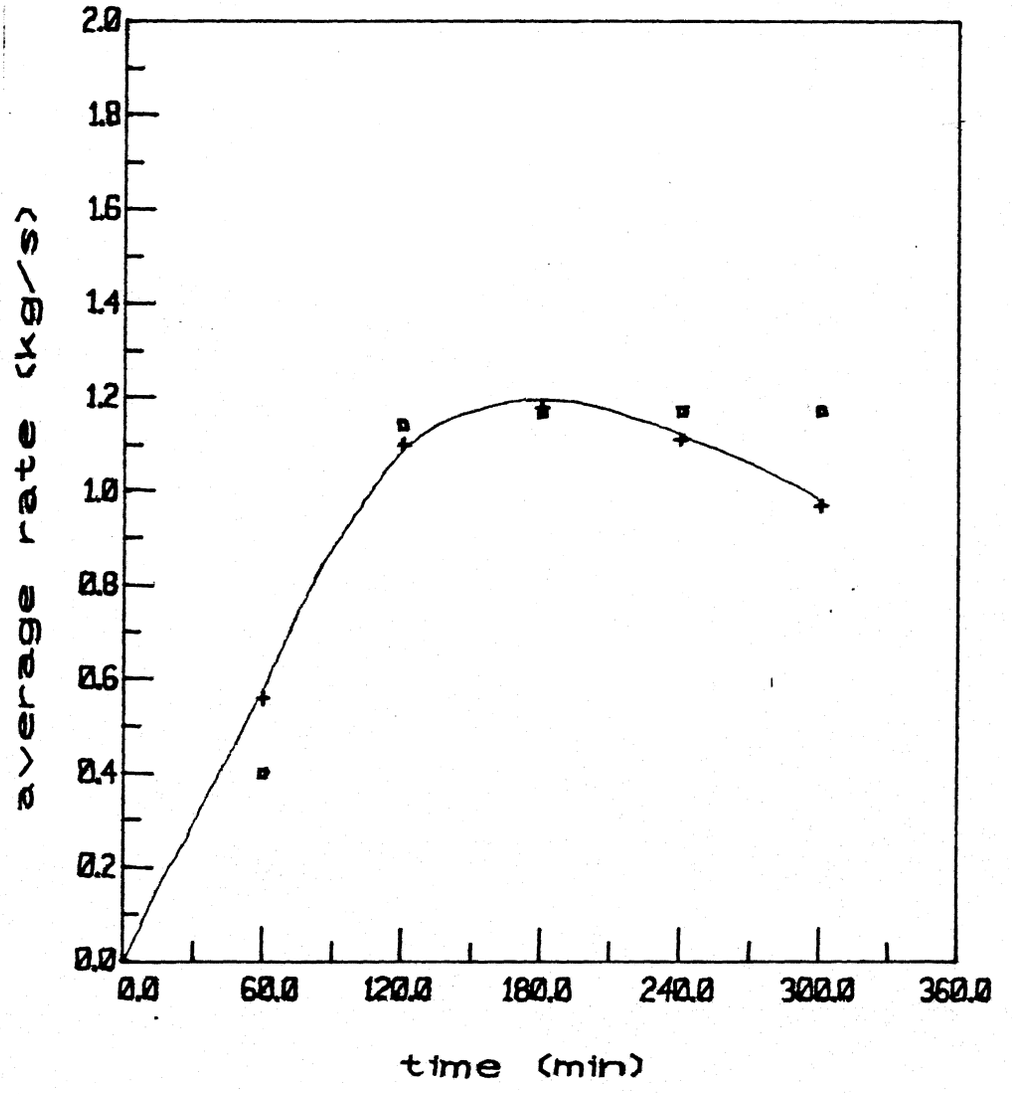

Fig 4.8b Comparison of polymerization rate between experimental data and model prediction for run 2

□, experimental data ; —— model

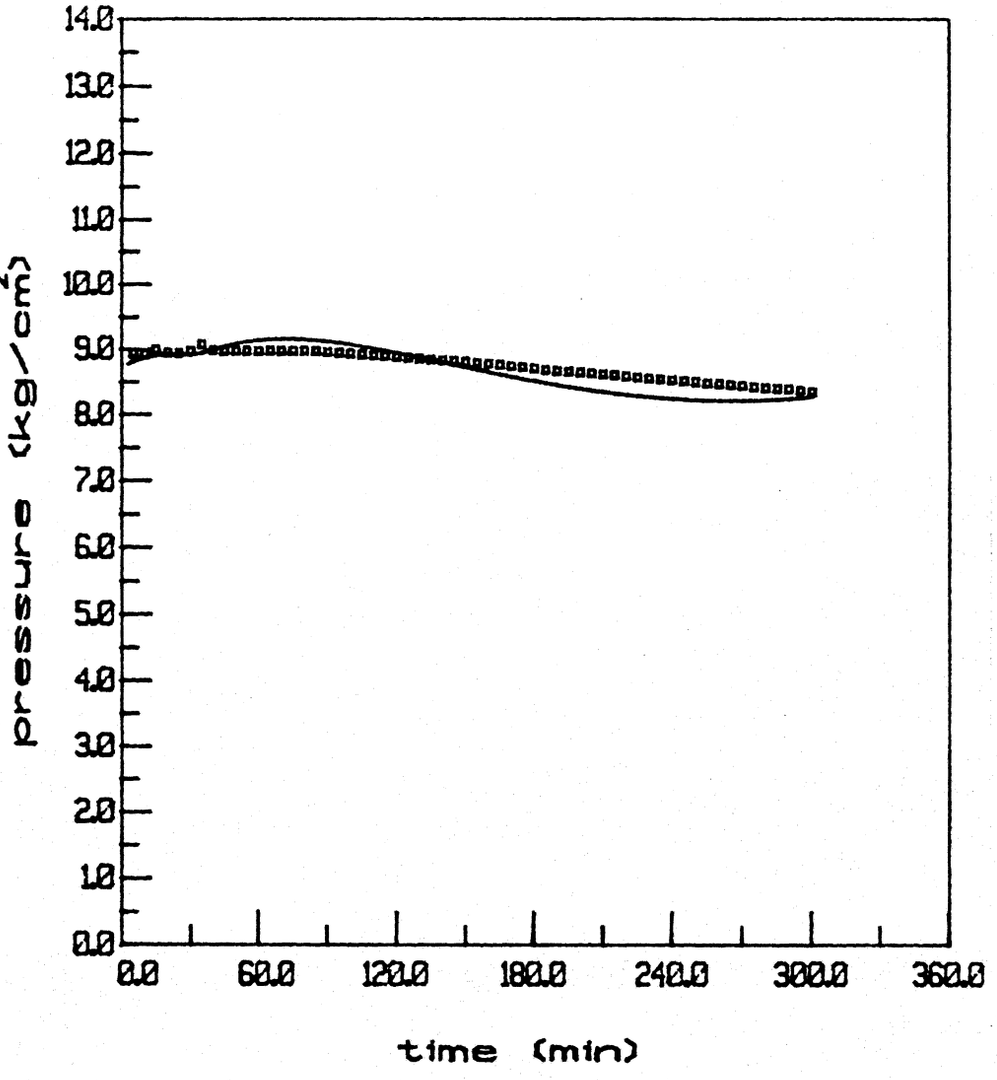

Fig 4.9a Comparison of pressure profile between experimental data and model prediction for run 1

□, experimental data ; —— model

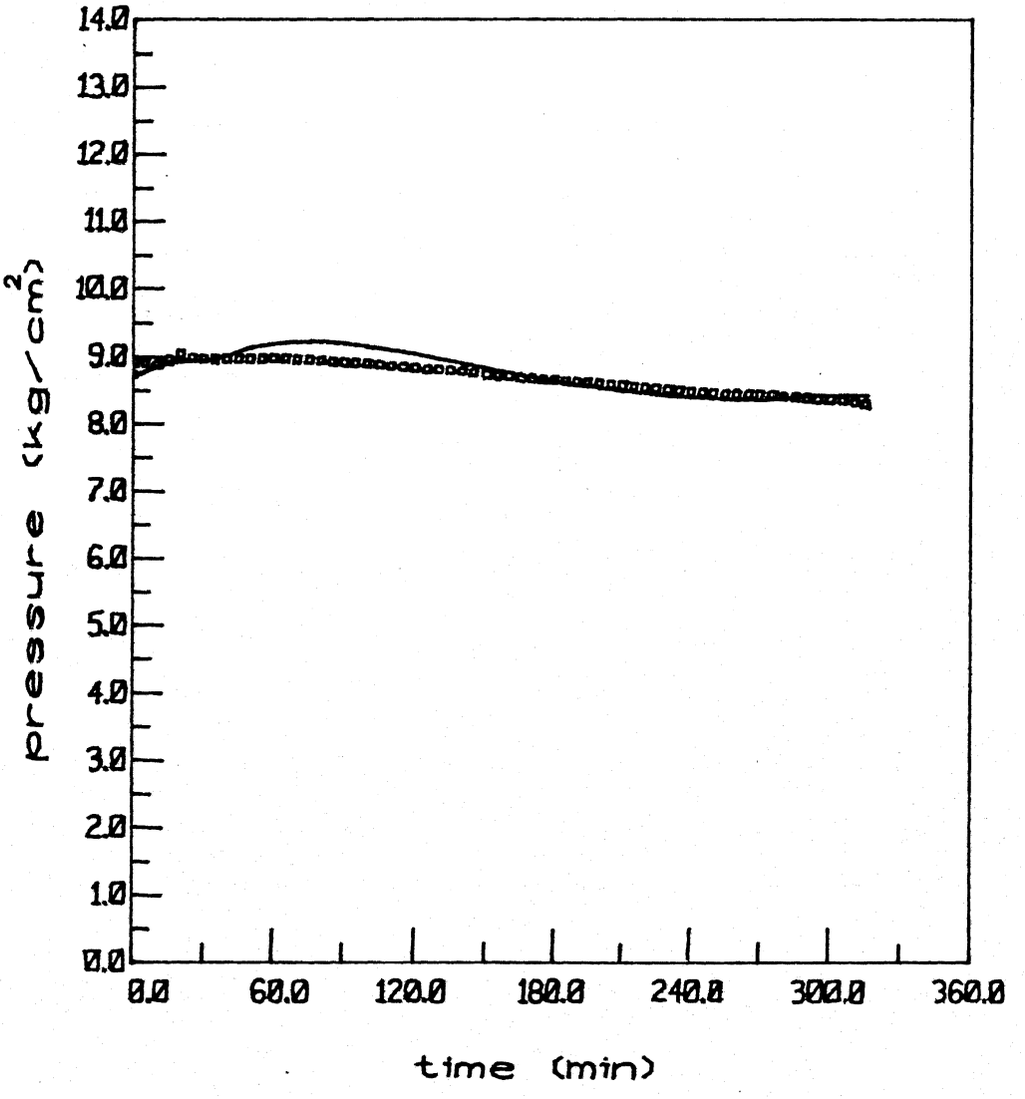

Fig 4.9b Comparison of pressure profile between experimental data and model prediction for run 2

□, experimental data ; —— model

the polymer phase. After solving the state equations forward, the Hamiltonian is set up as given in Chapter 3 and the adjoint equations (3.12) are integrated backwards. Then, the temperature profile is updated using equation (3.16). To attain the convergence quickly optimal value of ϵ is calculated at every iteration by simplex technique.

Optimization Result vs Industrial Result

The optimized rate profile has been found to be fairly flat which is shown in Fig 4.10. In this case the heat release is uniform and at the maximum cooling capacity. By operating the reactor along optimal temperature profile a 10% saving in reaction time can be achieved. The comparison of two conversion histories are shown in Fig 4.11. The corresponding reactor operating temperatures are shown in Fig 4.12.

Molecular Weight Averages

The cumulative molecular weight averages for the optimal temperature policy condition are little less than that of industrial run. This is shown in Fig 4.13. The corresponding polydispersity index (PDI) is shown in Fig 4.14. It has been found that for industrial run PDI is around 2.05 where as for the optimal temperature condition it is around 2.1.

Short and Long Chain Branching Characteristics

The formation of long chain branches (LCB) per thousand monomer units both for the industrial and optimal temperature policy run have been found to be very negligible. On the other hand, the formation of short chain branches (SCB) is appreciable. For the optimal temperature policy run it is slightly higher than for industrial case. This is shown in Fig 4.15.

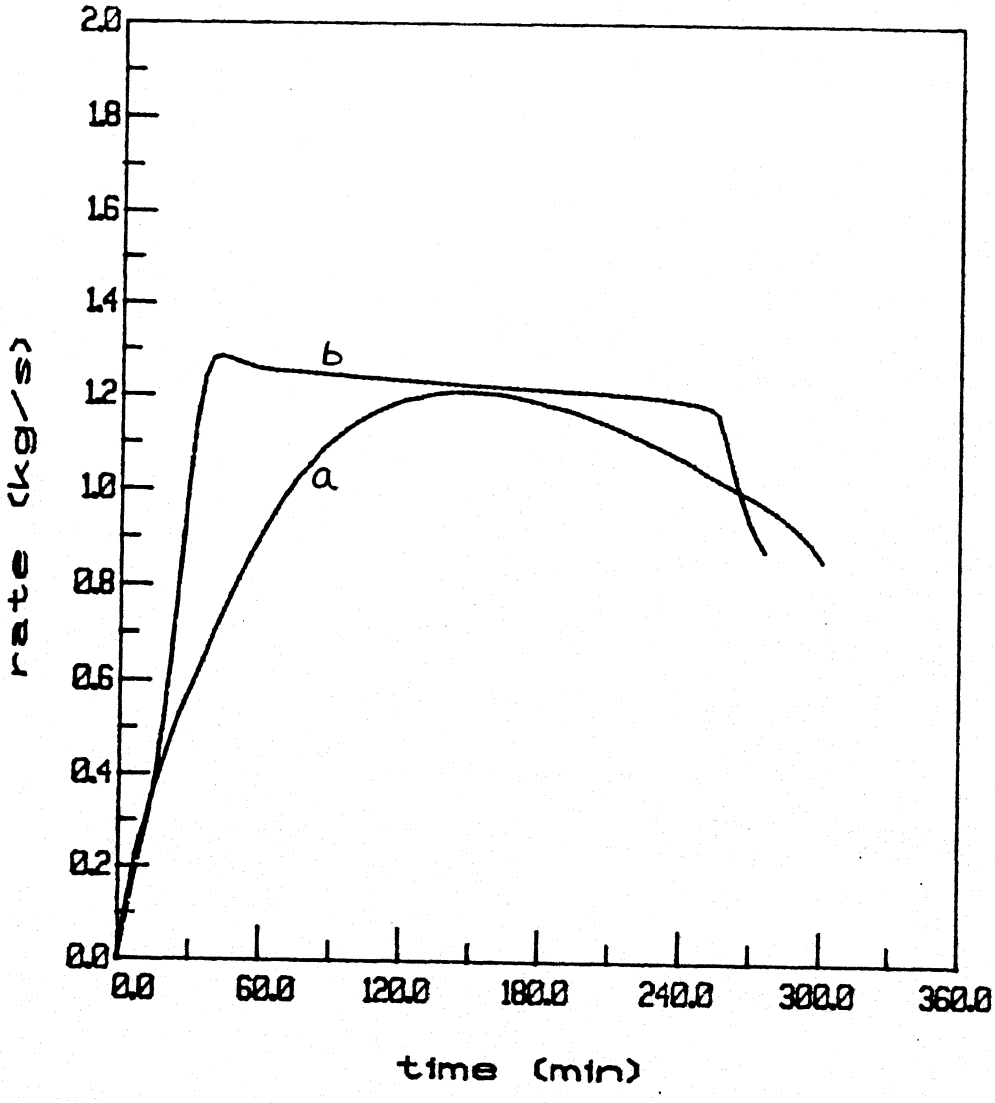

Fig 4.10 Comparison of rate profile

a) industrial rate profile

b) optimized rate profile

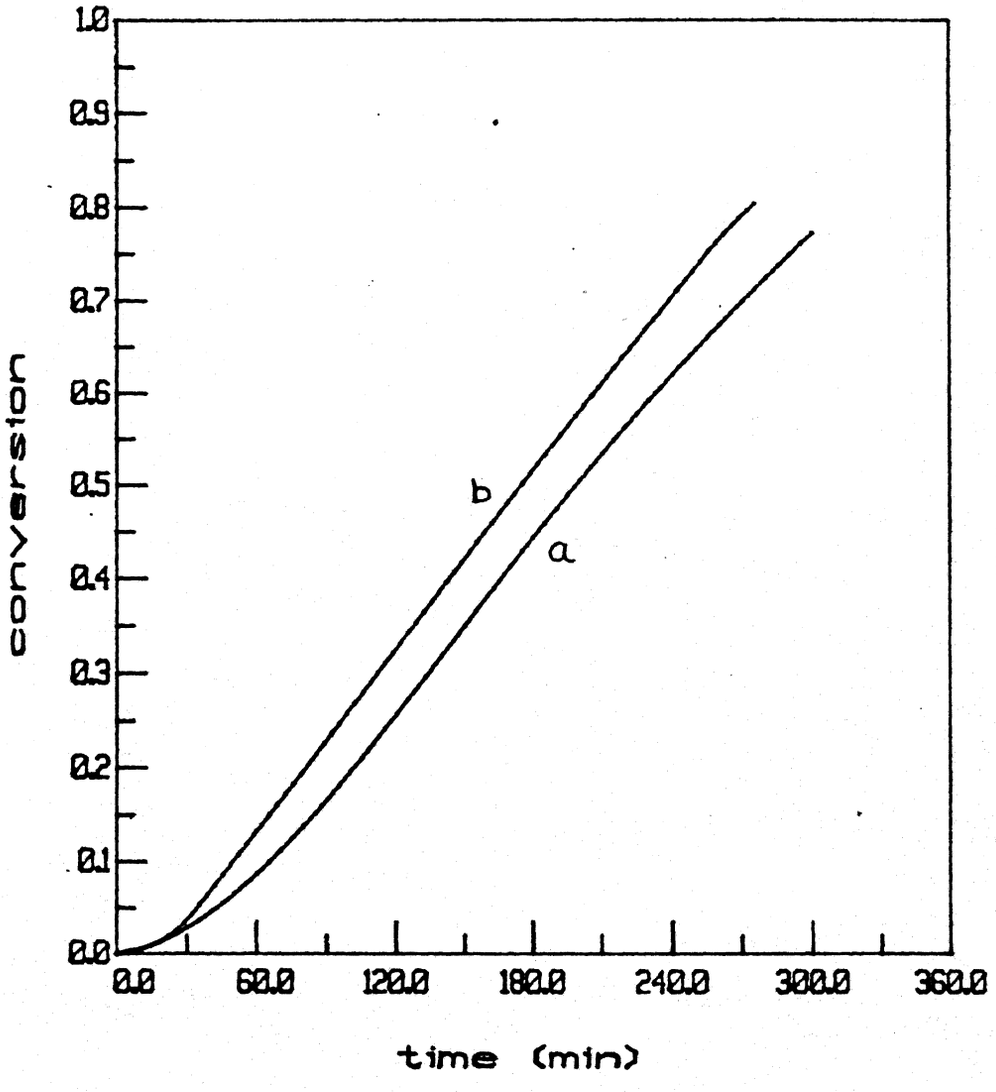

Fig 4.11 Comparison of conversion history

a) industrial conversion history

b) optimized conversion history

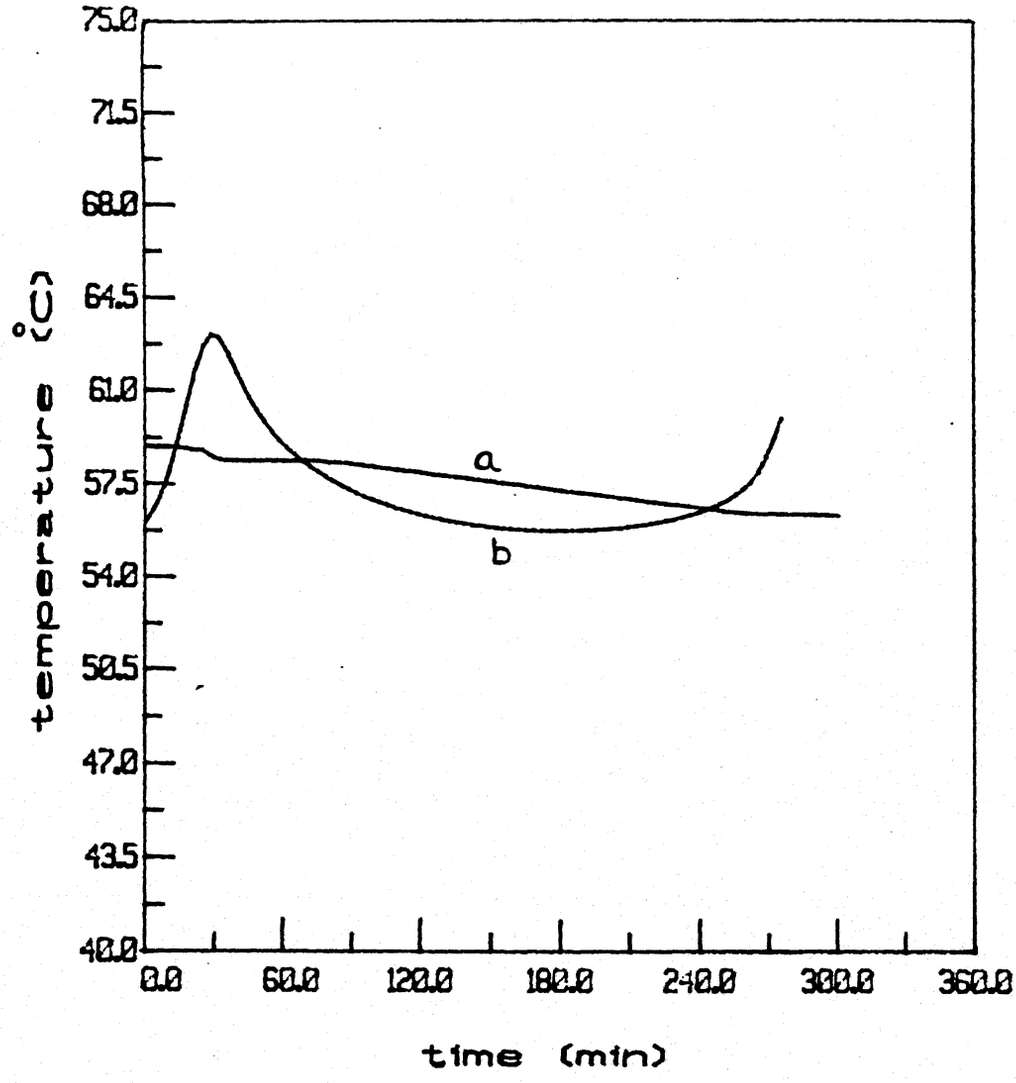

Fig 4.12 Comparison of temperature profile

a) industrial temperature profile

b) optimal temperature profile

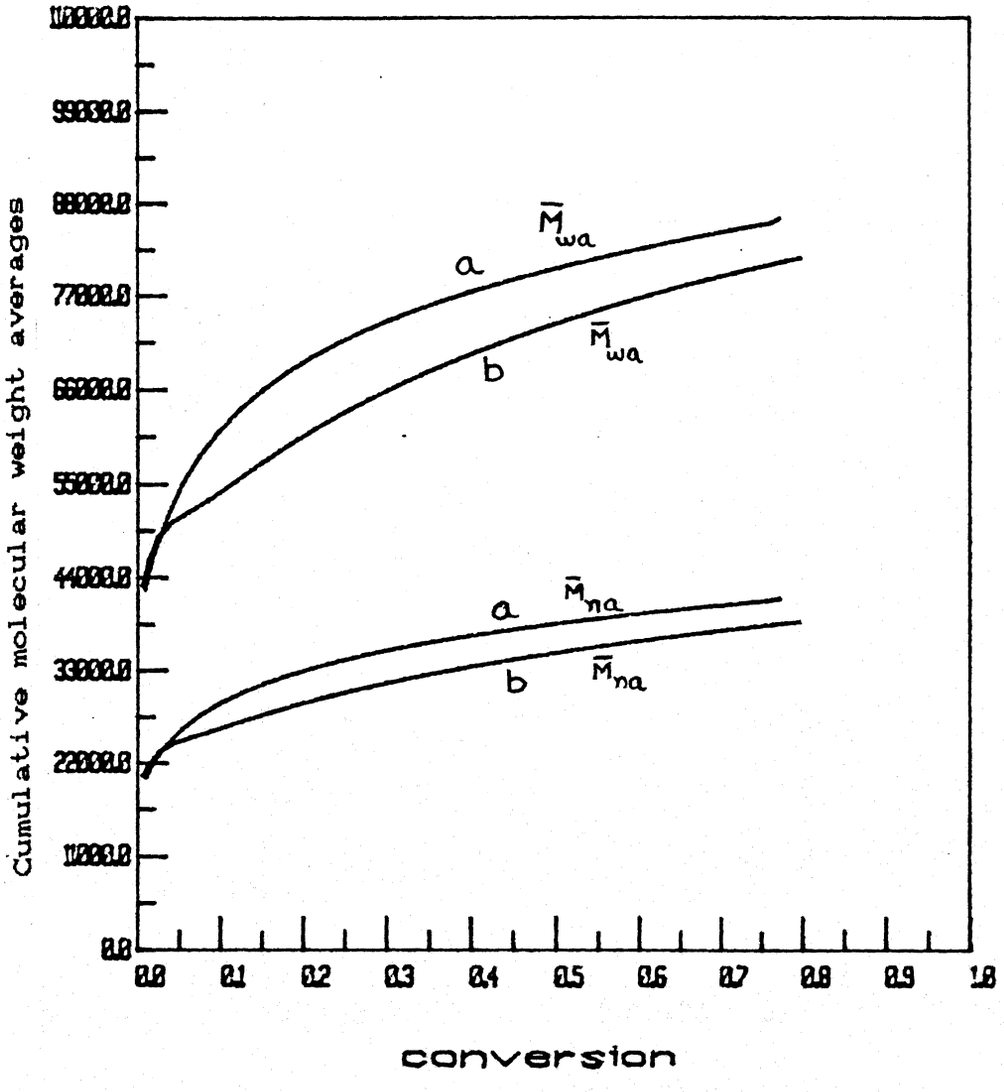

Fig 4.13 Comparison of cumulative molecular weight averages

a) industrial molecular weight averages

b) optimal temperature policy molecular weight averages

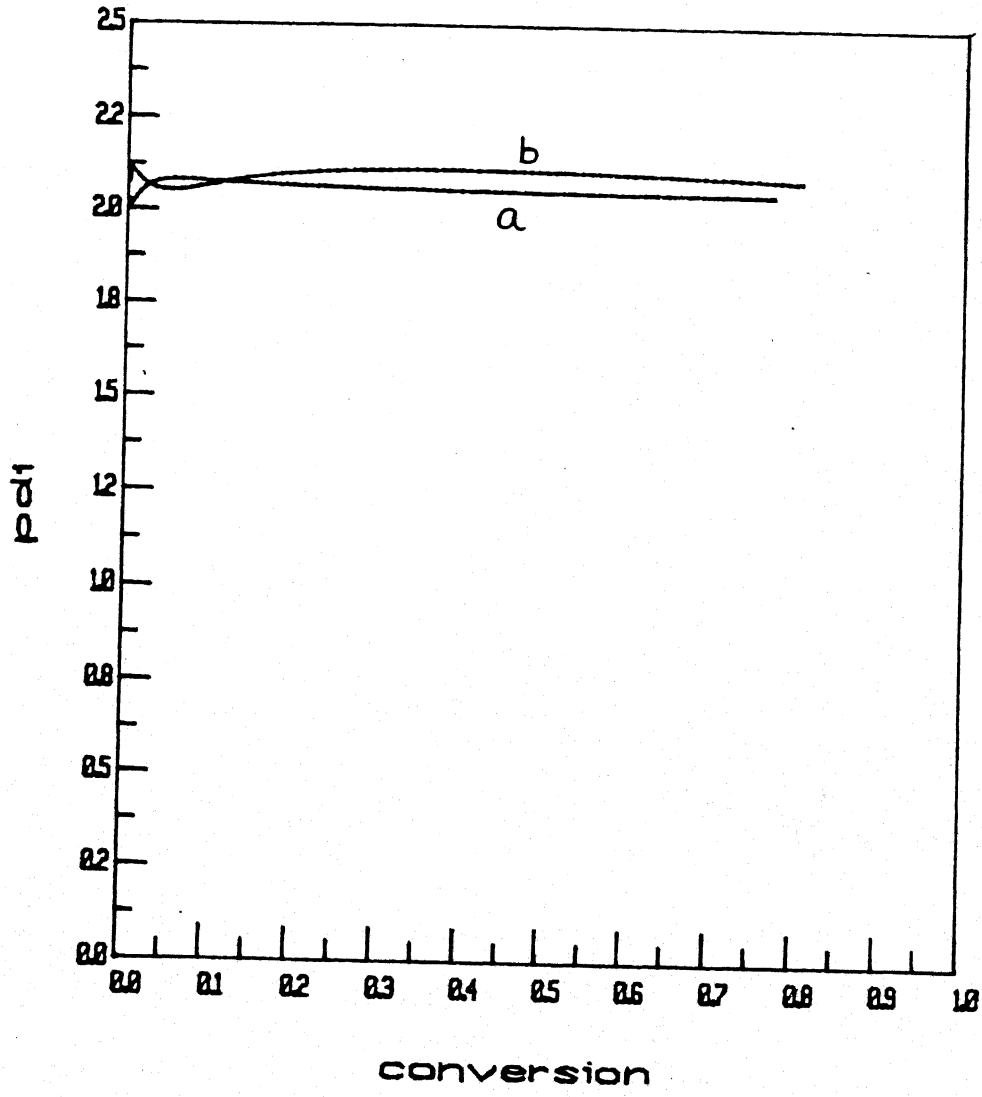

Fig 4.14 Comparison of polydispersity index

a) industrial PDI

b) optimal temperature policy PDI

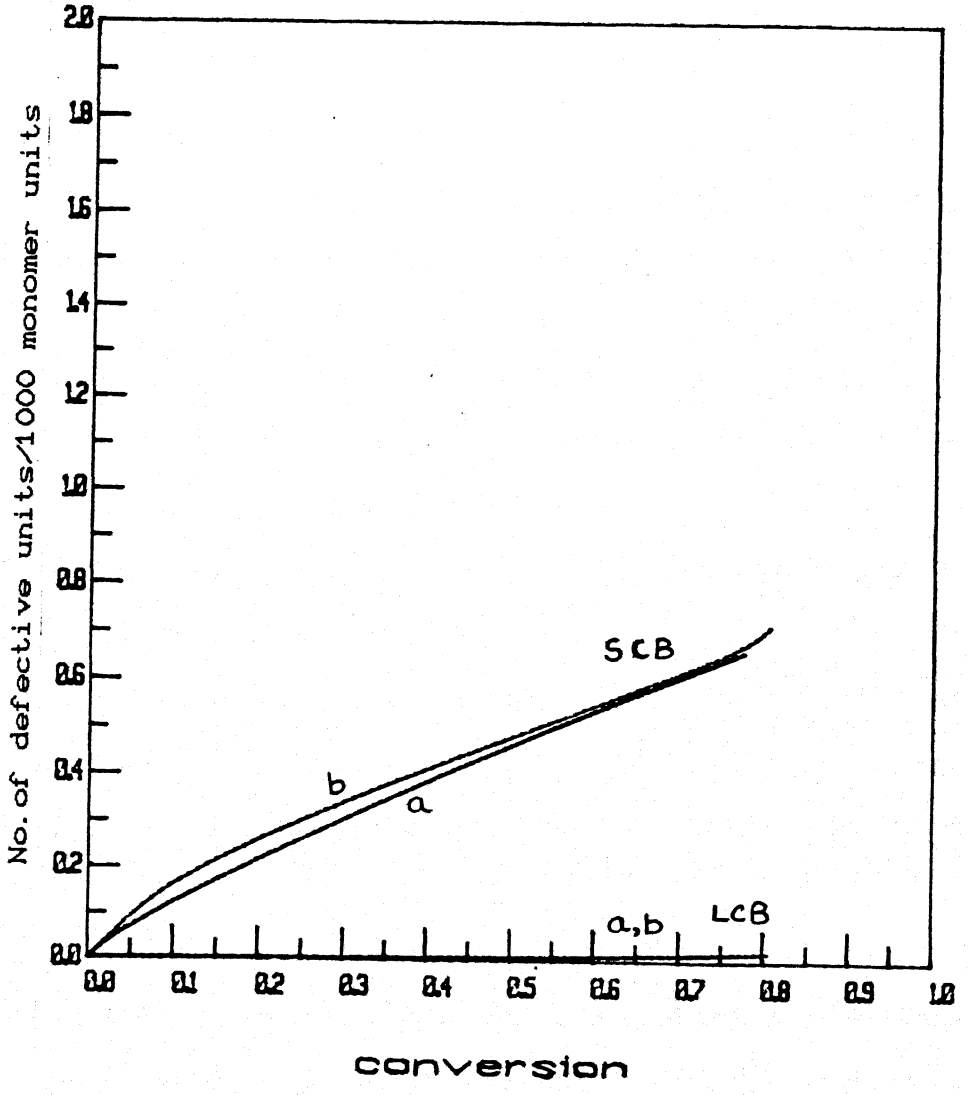

Fig 4.15 Comparison of short and long chain branching characteristics

a) industrial SCB & LCB

b) optimal temperature policy SCB & LCB

4.3 Heat Transfer Coefficients Results

To estimate the various heat transfer coefficients, the energy balance equations in Chapter 2 have been reorganised and given in Appendix II. In this system of equation the unknowns are jacket side heat transfer coefficient h_{ja}, reactor side heat transfer coefficient h_{in}, and baffle side heat transfer coefficient h_{bf}. The known variables are T_{ja}, T_{bf} and T.

Closed Loop Real Time Optimization (CLRTO) technique suggests to solve the five simultaneous equations coupled with an optimization technique to estimate the unknown parameters [30]. First initial values for these parameters are assumed and then the residuals of the simultaneous equations are driven to zero. The calculated variables like T, T_{ja} and T_{bf} are compared with the experimental data. If the values does not match, the parameter values are updated by using an optimization technique.

Since the coolant flow rate, inlet and outlet temperature of the coolant in the jacket is constant over the time we have fixed h_{ja} at 40.0 $W/dm^2.K$. This value has been obtained by trial and error method.

Since we have fixed h_{ja} we are left with two unknown parameters h_{bf} and h_{in}. The initial values for these parameters have been assumed as 40.0 and 20.0 $W/dm^2.K$ respectively. With these values the equations have been solved simultaneously using NAG routine C05NBF. The parameters are then updated using NAG routine E04CCf, Simplex optimization technique.

The results are shown in Table 4.5. The reactor inside heat transfer coefficient h_{in} thus estimated found to vary between 9.5 - 10.8 $W/dm^2.K$ whose value is close to the literature value 11.5

$W/dm^2.K$ [16]. h_{in} remains uniform through out the reaction time because continuously water is added into the reactor which keeps the mass slurry. The agitator power consumed during reaction remains almost uniform as per the industrial data. This shows that the viscosity of the medium does not rise significantly as polymerization proceeds. h_{bf} has been found to vary with time because the coolant flow rate varies with time.

Table 4.5 Heat transfer coefficients result

TIME	T_{ja} (C)	T_{bf} (C)	T (C)
40	33.34000	37.69000	58.36990
45	33.38000	44.24000	58.36000
50	33.42000	47.50000	58.36990
55	33.44000	44.64000	58.36000
60	33.46000	41.02000	58.36000
65	33.50000	38.15000	58.38000
70	33.51000	37.02000	58.36000
75	33.48000	34.72000	58.29990
80	33.47000	32.69000	58.29990
85	33.45000	32.55000	58.24000
90	33.42000	31.64000	58.18990
95	33.38000	30.46000	58.13000
100	33.35000	30.62000	58.08000
105	33.32000	29.60000	58.02000
110	33.28000	30.32000	57.97000
115	33.24000	30.74000	57.93000
120	33.21000	30.87000	57.84990
125	33.19000	30.81000	57.79990
130	33.16000	31.58000	57.75000
135	33.13000	31.48000	57.70000
140	33.11000	31.20000	57.63990
145	33.10000	31.13000	57.59000
150	33.07000	31.05000	57.52000
155	33.06000	31.35000	57.47990
160	33.07000	31.96000	57.41990
165	33.08000	32.45000	57.36000
170	33.09000	32.24000	57.29990
175	33.09000	30.46000	57.22990
180	33.07000	33.06000	57.18000
185	33.06000	31.83000	57.13990
190	33.04000	32.44000	57.09000
195	33.01000	32.38000	57.02990
200	32.98000	32.04000	56.97000
205	32.95000	32.11000	56.91990
210	32.92000	32.28000	56.86000
215	32.89000	32.17000	56.79990
220	32.87000	32.49000	56.74000
225	32.86000	31.82000	56.70000
230	32.84000	31.70000	56.65000
235	32.81000	31.97000	56.59990
240	32.78000	31.15000	56.54990
245	32.76000	30.77000	56.47000
250	32.73000	31.28000	56.43000
255	32.72000	30.96000	56.40000
260	32.70000	30.68000	56.38990
265	32.67000	29.87000	56.38000
270	32.63000	28.73000	56.36990
275	32.60000	28.01000	56.36990
280	32.57000	27.38000	56.36000
285	32.54000	27.22000	56.34990
290	32.51000	28.09000	56.34000
295	32.49000	29.87000	56.31990

TIME	h_{bf}	h_{in}
40	4.10000	9.53291
45	10.10000	9.86836
50	9.50000	9.94772
55	16.20000	10.04072
60	14.00000	10.02189
65	21.00000	9.95099
70	15.00000	10.02066
75	27.00000	10.11341
80	26.00000	10.27955
85	26.00000	10.17785
90	27.00000	10.13273
95	28.00000	10.07891
100	33.00000	10.05702
105	38.00000	10.03902
110	41.00000	9.98032
115	37.00000	9.89230
120	39.00000	9.92289
125	42.00000	9.88665
130	40.00000	9.83645
135	41.00000	9.81968
140	41.00000	9.77907
145	42.00000	9.82238
150	42.00000	9.78052
155	42.00000	9.77681
160	41.00000	9.81816
165	41.00000	9.86909
170	42.00000	9.95907
175	41.00000	9.97349
180	40.00000	9.90194
185	42.00000	9.90917
190	42.00000	9.89632
195	42.00000	9.86149
200	42.00000	9.80785
205	40.00000	9.76768
210	42.00000	9.75300
215	42.00000	9.71542
220	42.00000	9.67740
225	42.00000	9.69553
230	43.00000	9.67286
235	43.00000	9.62655
240	43.00000	9.59385
245	43.00000	9.59194
250	43.00000	9.51848
255	43.00000	9.51786
260	43.00000	9.47599
265	43.00000	9.41290
270	43.00000	9.33206
275	43.00000	9.27774
280	43.00000	9.21239
285	43.00000	9.13349
290	43.00000	9.06105
295	43.00000	8.98963

TIME	$\dot{m}_{ja}$	$\dot{m}_{bf}$
40	60796.11528	1469.56528
45	60768.75417	2618.73194
50	60741.66667	2270.69861
55	60850.83750	4016.58375
60	60686.67083	3737.50042
65	60276.52778	5518.73611
70	60331.25000	4355.88889
75	60632.22222	7507.86153
80	61124.44861	7625.51431
85	60850.83750	7693.91708
90	60823.75000	8071.50042
95	60796.11528	8572.23611
100	60823.75000	9510.72222
105	60823.75000	10892.43097
110	60823.75000	11302.87500
115	60768.75417	10290.51389
120	60850.83750	10876.04167
125	60823.75000	11401.37500
130	60796.11528	10782.98653
135	60823.75000	11231.70875
140	60768.75417	10947.15319
145	60850.83750	11373.98653
150	60823.75000	11289.19444
155	60850.83750	11062.09722
160	60796.11528	10843.18097
165	60823.75000	10621.55597
170	60905.83333	11081.25000
175	60850.83750	11220.79167
180	60796.11528	10148.23611
185	60768.75417	11130.50000
190	60796.11528	10919.79208
195	60823.75000	10758.36153
200	60796.11528	10698.16708
205	60796.11528	10375.33333
210	60823.75000	10977.25042
215	60823.75000	11026.50042
220	60796.11528	10668.09722
225	60823.75000	11144.15319
230	60823.75000	11294.66667
235	60823.75000	11261.80597
240	60796.11528	12120.94486
245	60823.75000	11710.52819
250	60823.75000	11349.36153
255	60823.75000	11650.33375
260	60823.75000	12017.00000
265	60796.11528	12848.75042
270	60796.11528	13874.79208
275	60850.83750	14104.62542
280	60850.83750	14285.20875
285	60823.75000	14244.19444
290	60850.83750	12424.65319
295	60850.83750	10525.81944

CHAPTER 5

CONCLUSIONS AND SUGGESTIONS

5.1 Conclusion

A multi-phase mathematical model has been presented for free radical suspension polymerization of VCM in a batch reactor. This model takes care of precipitation of monomer from monomer phase into other phases and predicts pressure drop in the reactor. We have assumed here that VCM vapor obeys ideal gas law. Apart from pressure prediction this model also predicts polymerization rate, cumulative molecular weight averages and long and short chain branches characteristics.

There are several parameters in the model. The sensitivity of these model parameters to polymerization rate and pressure profile has been studied. For this purpose, by simulation experience we fixed the upper and lower bound values for each parameter and sensitivity analysis has been investigated in that domain. Based on our sensitivity analysis we found that four parameters viz., monomer partition coefficient γ_{12}^{M}, initiator partition coefficient γ_{12}^{I}, radical diffusivity D_{12}^{R} and initiator efficiency ratio β were very sensitive to polymerization rate but insensitive to pressure profile. On the other hand, we found monomer interphase mass transfer coefficient k_{M45}^{M} was sensitive to pressure profile but insensitive to polymerization rate.

Among these parameters γ_{12}^{M} is the most sensitive parameter which determines the rate profile. We found by increasing the monomer concentration in the polymer phase the rate could be enhanced. This suggests a semi-batch mode of operation with

respect to monomer after critical conversion to keep the monomer concentration in the polymer phase as high enough to prevent a fall in pressure. This would also minimize the formation of defective structures thus improving the thermal stability of PVC. We could not investigate this semi-batch mode operation as we ran out of time.

Having found out the sensitive parameters, we estimated these value using industrial data. The Simplex optimization method has been used to estimate the value of these parameters. We estimated the parameters for seven such industrial run and an average value has been taken for each parameter.

To utilise the maximum cooling capacity of the reactor, we found an optimal temperature policy using Pontryagin's Continuous Minimum Principle. When the reactor is operated along this optimal temperature policy a 10% saving in time is realised. Although there is a increase in productivity this has it's own drawbacks. By operating along optimal temperature policy the cumulative molecular weight averages decreases slightly which in turn may affect the grade of PVC resin. If this fall is not acceptable for the end use of PVC it can be incorporated as a constraint.

All the three heat transfer coefficients (h_{ja}, h_{bf}, h_{in}) in the energy balance have been estimated using industrial data. The estimated heat transfer coefficient h_{in} lies close to the reported value in the literature.

5.2 Suggestions for future work

i) To use multiple initiator systems for achieving flatter heat release. To utilise the maximum cooling capacity of the reactor it is necessary to keep the rate profile flat. The dominating approach to this problem is to use a combination of rapid and slow initiators.

ii) Agitation is very important in the suspension PVC process in that it determines the monomer droplet size. It governs the stability of the suspension during polymerization and particle size of the product formed. It also plays an important role in determining product properties such as porosity and bulk density. Also, it has a significant effect on the reactor inside heat transfer coefficient. In general more agitation will increase inside heat transfer coefficient and, hence, the overall heat transfer coefficient. Therefore modelling related to agitation is of prime importance.

iii) To incorporate the quantitative relationship between product characteristics (like porosity, particle size distribution, crystallinity, intrinsic viscosity), hydrodynamic and operating conditions of the batch reactor.

iv) To operate the reactor in a semi-batch mode to maintain monomer concentration as high enough to prevent a drop in the operating pressure. This drop occurs nearly at critical conversion. Till critical conversion batch mode is followed and after switched to semi-batch mode to reduce the formation of defective structures, prevent thermal

instability and to prevent fall in the molecular weight of PVC. It is suggested to add monomer in the vapor phase continuously in the semi-batch mode so that the polymer particle sucks the monomer from vapor phase.

v) To use energy balance equation in the model to predict the reaction temperature. This is essential to control the reactor temperature along the optimal temperature profile.

References

1. Talamini, G., *J.Polym.Sci.*, (A-2)., **4**, 535 (1966).
2. Abdel-Alim, A.., Hamielec, A.E., *J.Appl.Polym.Sci.*, **16**, 783 (1972).
3. Ugelstad, J., Flogstad, H., Hertzberg, T.,Sund.E., *Makromol.Chem.*, **164**, 171 (1973).
4. Ugelstad, J., Mork, P.C., Hansen, F.K., *Pure Appl.Chem.*, 53 , 323 (1981).
5. Olaj.O.F., *J.Macromol.Sci.Chem*, A11, 1307 (1977).
6. Kuchnov, S.J., Bort, D.N., *Polym.Sci.USSR*, **15**, 2712 (1973).
7. Kelsall ,D.G., Maitland, G.C., Polymer Reaction Engineering, Reichert, K.H., Geiseler, W., Munich, Vienna, New York, 132 (1983).
8. Xie, T.Y., Hamielec, A.E., Wood, P.E., Woods, D.R., *J.Appl.Polym Sci.*, **43**, 1259 (1991).
9. Xie,T.Y., Hamielec,A.E., Wood, P.E., Woods, D.R., *J.Appl.Polym Sci.*, **34**, 1749 (1987).
10. Hamielec, A.E., Gomez-Vailland, R., Marten, F.L., *J.Macromol.Sci, -Chem.*, **17(6)**, 1005 (1982).
11. Xie, T.Y., Hamielec, A.E., Wood, P.E., Woods, D.R., *Polymer*, 32, 3, 548-552 (1991).
12. Xie, T.Y., Hamielec, A.E., Wood, P.E., Woods, D.R., *Polymer*, 32, 11, 2087 (1991).
13. Xie, T.Y., Hamielec, A.E., Wood, P.E., Woods , D.R., Chiantore, O., *Polymer*, 32, 9, 1699 (1991).
14. Sidiropolou, E., Kiparissides, C., *J.Macromol.Sci.*, A 27(3), 259 (1990).

15. Xie, T.Y., Hamielec, A.E., Wood, P.E., Woods, D.R., *Polymer*, 32, 6, 1098 (1991).

16. Lyle F.Albright and Yogendra Soni, *J.Macromol.Sci.-Chem*, A17(7), 1065 (1982).

17. Yogendra Soni and Lyle F.Albright, *J.Appl.Polym.Sci*, 36, 113 (1981).

18. Berens, A.R., *Polymer*, 18, 697 (1977).

19. Butters, G., (Edi), Particulate Nature of PVC, Applied Science Publishers Ltd., London (1982).

20. Glass, J.E., and Fields, J.W., *J.Appl.Polym.Sci.*, 16, 2269 - 2290 (1972).

21. Allsopp, M.W., *J.Appl.Chem.*, 53, 449 (1981).

22. Hofmann, E., and Kummert, I., *Plaste und Kautschuk*, 23(8), 56 (1976).

23. Cebollada, A.F., Schmidt, M.J., Farber, J.N., Capiati, N.J., and Valles, E.M., *J.Appl.Polym.Sci*, 37, 145 (1989).

24. Smallwood, P.V., *Polymer*, 27, 1609 (1986).

25. Maranin, V.V., Bort, D.N., Zhieltsov, V.V., Kuchanov, S.I., Zvereva, G.F., Rybkin, E.P., *Polym.Sci.USSR*, 22, 261 (1980).

26. Davidson, J.A., Witenhofer, D.E., *J.Polym.Sci., Polymer Phys.*, Ed.18, 51 (1980).

27. Govindhakannan, J., M.Tech Thesis., 1 - 87 (1992).

28 Rajeev Mishra, and Vaibhav Tewari, B.Tech Project, 14 - 15 (1993)

29. Hjertberg, T., Sorik, E.M., *J.Macromol.Sci.-Chem*, A-17(6), 983 (1982).

30. Fatora, F.C., Ayala, J.S., Hydrocarbon Processing, 6, 65-66 (1992).

31. Indian Petrochemicals Corporation Ltd data.

APPENDIX I

Calculation for initiator distribution among three phases on initiator addition

Let the total flow rate of initiator be F_I. This amount gets distributed among three phases (monomer, polymer and skin phases) based on initiator partition coefficients between different phases. γ^I_{13} is taken as same as γ^I_{12}.

$$F_I = F_{I1} + F_{I2} + F_{I3} \qquad (I.1)$$

where F_{I1}, F_{I2}, and F_{I3} are the amount of initiator flowing into phase 1, phase 2 and phase 3 respectively. Let Δt be the time interval for integrating the state equations (2.8-2.19,2.40,2.41) We know

$$\gamma^I_{12} = \left[\frac{(I_1 + F_{I1}\Delta t)/V_1}{(I_2 + F_{I2}\Delta t)/V_2} \right] \qquad (II.2)$$

where I_1 and I_2 are the initiator amount already present in phase 1 and phase 2 before adding up further.

Also,

$$\gamma^I_{13} = \gamma^I_{12} = \left[\frac{(I_1 + F_{I1}\Delta t)/V_1}{(I_3 + F_{I3}\Delta t)/V_3} \right] \qquad (II.3)$$

Knowing F_I and γ^I_{12} we can solve the above three equations simultaneously to yield F_{I1}, F_{I2} and F_{I3}. I_1, I_2, I_3, V_1, V_2 and V_3 are obtained from while simulating the model.

APPENDIX II

Formulations for Heat Transfer Coefficients Estimation

$$R_1 = \dot{m}_{ja} C_w (T_{jai} - T_{jae}) + h_{ja} A_{ja} (T_{m1} - T_{ja}) - V_{ja} \rho_w C_w \frac{\Delta T_{ja}}{\Delta t}$$

$$R_2 = \dot{m}_{bf} C_w (T_{bfi} - T_{bfe}) + h_{bf} A_{bf} (T_{m2} - T_{bf}) - V_{bf} \rho_w C_w \frac{\Delta T_{bf}}{\Delta t}$$

$$R_3 = h_{in} A_{ja} (T - T_{m1}) - h_{ja} A_{ja} (T_{m1} - T_{ja}) - \rho_{mw} C_m V_{m1} \frac{\Delta T_{m1}}{\Delta t}$$

$$R_4 = h_{in} A_{bf} (T - T_{m2}) - h_{bf} A_{bf} (T_{m2} - T_{bf}) - \rho_{mw} C_m V_{m2} \frac{\Delta T_{m2}}{\Delta t}$$

$$R_5 = (-\Delta H) M_0 \frac{dx}{dt} - h_{in} A_{ja} (T - T_{m1}) - h_{in} A_{bf} (T - T_{m2})$$

$$- V_R \rho_r C_p \frac{\Delta T}{\Delta t} + H_a$$

where H_a is the heat developed by the agitation. It is estimated [16] that 90% of agitator power is converted into heat.

This open equation based model has been formulated to suit CLRTO (Closed Loop Real Time Optimization) technique [30]. R_1, R_2, R_3, R_4, and R_5 are the residuals of the simultaneous equations.

APPENDIX III

Quantisation of non - fickian diffusion of VCM in PVC [18]

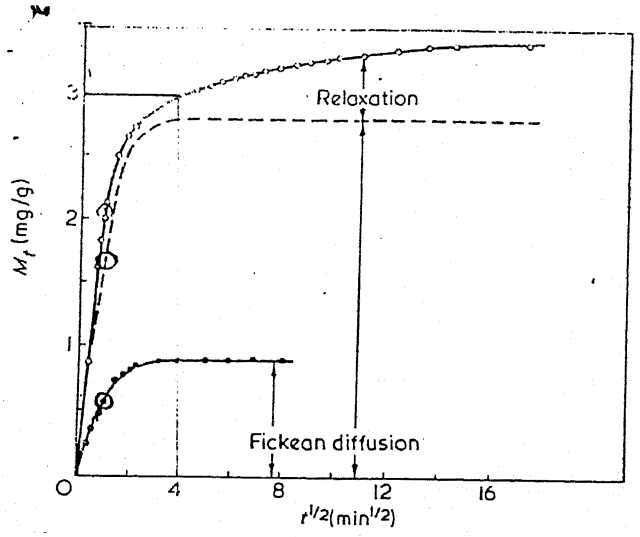

The above graph shows the fickian and non - fickian diffucion process of VCM in PVC.

The fickian diffusion of VCM in PVC can be calculated as follows,

$$\frac{M_t}{M_\infty} = 1 - (6/\pi^2) \sum_{n=1}^{\infty} (1/n^2) \exp(-4D_{12}^M n^2\pi^2 t/d^2) \qquad \text{(III.1)}$$

where M_t is the weight of penetrant entering or leaving the sphere in time t after an instantaneous change in surface concentration, M_∞ is the total weight change after infinite time at the new surface concentration, n is the series of integers, D_{12}^M is the diffusion coefficient, and d is the diameter of the sphere.

For calculating fickian diffusion consider a point on fickian diffusion curve. At $t^{0.5} = 4.0 min^{0.5}$, $M_t/M_\infty = 0.99$. The diameter of particle is $d = 4.47*10^{-5}$dm. Substituting these

values in eqn (III.1) we get $D_{12}^{M} = 2.0*10^{-13}$ dm^2/sec.

For quantising the non - fickian diffusion process, let us consider a point on the non - fickian curve in the graph shown here.

At $t^{0.5} = 4\ min^{0.5}$, $M_t = 3.0$ mg/gm , $M_\infty = 3.4$ mg/gm

Substituting these values in eqn (III.1)

we get $D_{12}^{M} = 8.66*10^{-14}$ dm^2/sec.

APPENDIX IV

Stability of Computational Technique

The stability of numerical technique used in optimization problem has been investigated by reducing the step length of time Δt from 200 sec to 100 and 50 sec. The effect of this reduction on optimal temperatue profile is shown below. From this graph one can conclude that the present step length Δt = 200 sec is a good increment in time.

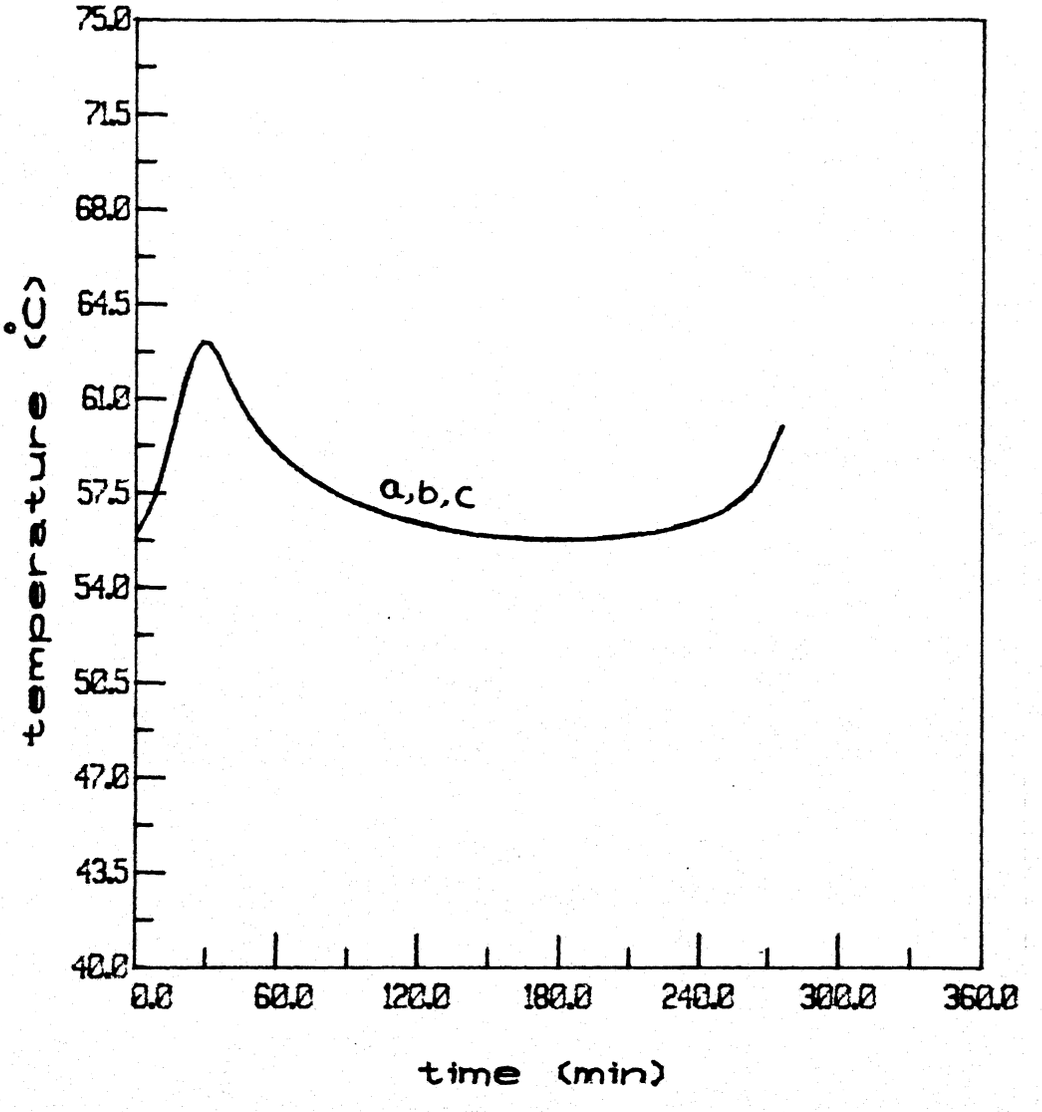

Fig IV.1 Effect of step length Δt

a) Δt = 200 b) Δt = 100 c) Δt = 50 sec.